Adrenergic Regulation of Cardiac $Ca_V1.2$ via Direct Phosphorylation and the GTPase RAD

Liam Hovey

A dissertation

submitted in partial fulfillment of the

requirements for the degree of

Doctor of Philosophy

University of Washington

2021

Reading Committee:

William Catterall, Chair

Yasemin Sancak

Qinghang Liu

Program Authorized to Offer Degree:

Pharmacology

University of Washington

Abstract

Adrenergic Regulation of Cardiac $Ca_V1.2$ via Direct Phosphorylation and the GTPase RAD

Liam Hovey

Chair of the Supervisory Committee:
William A. Catterall, PhD
Department of Pharmacology

Dysregulation of the cardiac fight-or-flight response has been linked to chronic heart failure and arrhythmic disorders. The L-type calcium channel $Ca_V1.2$ has a central role in mediating the cardiac fight-or-flight response, but the precise molecular mechanisms that transduce adrenergic stimulation to increased cardiac output are not completely characterized. This work seeks to address fundamental mechanistic questions related to the regulation of $Ca_V1.2$ during the cardiac fight-or-flight response, and thus lay the groundwork for next-generation therapies targeting the β-adrenergic-$Ca_V1.2$ signaling axis. I have specifically focused on a critical question in the field: is $Ca_V1.2$ activity primarily regulated by direct phosphorylation during the fight-or-flight response, or through other molecular mediators? I report here that direct phosphorylation of the C-Terminal Domain of $Ca_V1.2$ has an important role in cardiac function and $Ca_V1.2$ activity, and that the small GTPase RAD co-regulates the channel alongside direct

phosphorylation. These findings indicate that the molecular mechanism of the cardiac fight-or-flight response is characterized by convergence of the direct phosphorylation and RAD pathways to co-regulate $Ca_V1.2$ activity.

TABLE OF CONTENTS

LIST OF FIGURES

LIST OF TABLES

ACKNOWLEDGEMENTS

Deepest thanks to my mentor, Dr. Catterall, and the members of the Catterall lab who trained and supported me and thus facilitated the work described herein. My gratitude also to the Liu laboratory for sharing their time and expertise on the *in vivo* mouse cardiac experiments, especially to Xiaoyun Guo, who dedicated countless hours to surgeries and echocardiography in support of my thesis work. Finally, thank you to my thesis committee, Dr. Catterall, Dr. Sancak, Dr. Liu, and Dr. McKnight for guiding this work and my PhD studies.

DEDICATION

I dedicate this work to my grandmother, Patricia Harper, who has supported my education in ways innumerable, and whose selflessness, lifelong curiosity, and integrity are a model for us all.

Chapter 1. An Introduction to $Ca_V1.2$ and the Cardiac Fight-or-Flight Response

The cardiac fight-or-flight response is a dramatic, familiar physiological phenomenon characterized by a racing, pounding heart beat. Evoked by stress, fear, or anticipation, variants of this reflex are observed throughout the metazoans.[1] Scientists and physicians have long sought to understand the biological underpinning of the cardiac fight-or-flight response, since many disease processes are intertwined with the cardiac adrenergic axis.[2] In fact, one of the earliest clinical applications of exogenous epinephrine, shortly after its isolation 125 years ago, was in the treatment of a case series of patients with "neurotic heart" (an arrhythmic disorder reminiscent of the modern supraventricular tachycardia).[3-5] In the decades since its discovery, epinephrine and other biogenic catecholamines have gained widespread use in cardiological, emergency, and intensive care applications.[6-8] A further testament to the importance of research into the cardiac flight-or-flight axis emerged in 1958 with the development of β-adrenergic *ant*agonists, which inhibited the fight-or-flight response by blocking the action of adrenergic receptors in cardiac tissue.[9] The subsequent introduction of β-adrenergic antagonists in human clinical settings reshaped the standard-of-care for a number of deadly diseases, ranging from acute coronary syndrome to heart failure to tachyarrhythmias. β-adrenergic antagonists, versatile inhibitors of the cardiac fight-or-flight response, thus became one of the great, lasting successes of modern cardiovascular pharmacology.[10, 11]

Despite the remarkable impact adrenergic modulators have had on cardiovascular medicine, much of the molecular and atomic detail of the cardiac β-adrenergic axis remains inadequately characterized or shrouded in controversy.[12] A more extensive characterization of

cardiac fight-or-flight signaling, particularly the signaling pathways that bridge the cAMP-mediated stimulatory mechanism to upregulation of constituents within the calcium cycle and myocardial contraction, promises to offer novel therapeutic targets for diverse disorders involving the cardiac adrenergic system.

1.1 Cardiac Ca^{2+} Signaling And Adrenaline: A Century of Perspective

Our understanding of the fight-or-flight response, particularly the cardiovascular aspect, improved dramatically in the late 19th century with the isolation and characterization of adrenal hormones.[13, 14] In 1895, two separate laboratories described in detail the effects of "suprarenal extract" (clarified, homogenized adrenal tissue) on explanted animal hearts.[3, 4] The resulting findings, that heart rate and myocardial contractile force could be regulated by potent circulating stimulatory factors, formed the basis for a century of increasingly detailed characterizations of the pathways that govern – and the pathologies that implicate - the cardiac fight-or-flight axis.

Deeper insight into the molecular mechanisms that give rise to the cardiac fight-or-flight response was attained as electrophysiological techniques became more widely disseminated during the mid-20th century.[15, 16] Ahlquist described α and β-adrenergic receptors as the mediators of the adrenergic response in the cardiovascular system in 1948. Otsuka demonstrated in 1958 that action potentials in isolated sheep heart ventricular myocytes acquired higher amplitudes and altered kinetic characteristics following exposure to epinephrine, and Reuter subsequently demonstrated that calcium permeability in guinea pig atria was increased in the presence of epinephrine.[17-19] Tsien observed in 1972 that cAMP mediated alterations in the cardiac action potential following cardiomyocyte stimulation with catecholamines.[20]

As the contemporary cardiac molecular fight-or-flight paradigm developed, the focus of investigation into the cardiac adrenergic response shifted to downstream targets, and detailed discussion emerged on the importance of phosphorylation sites that carry the fight-or-flight signal from the cardiomyocyte membrane to the molecular machinery of the calcium cycle, the contractile apparatus, and the nucleus.[12, 21]

Over the past two decades, mechanisms that had originally been discovered in the skeletal muscle calcium channel $Ca_V1.1$ were identified as being relevant to the closely-related cardiac channel $Ca_V1.2$.[22-26] In particular, the C-Terminal tail (CTD) of $Ca_V1.2$ was shown to undergo proteolysis and phosphorylation in a manner that dramatically altered conduction characteristics. This phosphorylation was found to be cAMP-dependent protein kinase A (PKA) dependent, indicating that post-translational modification of the $Ca_V1.2$ CTD, and thus cardiac sarcolemmal calcium current, varied according to cardiac adrenergic tone.[27-30] These findings suggested a mechanistic link, with residue-level resolution, between the β-adrenergic axis and the transmembrane calcium current that initiated excitation-contraction coupling. In recent years, the role of direct phosphorylation of $Ca_V1.2$ in the cardiac adrenergic response has been challenged with the characterization of additional PKA-sensitive mediators that also appeared to relate adrenergic stimulation to increased $Ca_V1.2$ activity, particularly through the $Ca_V\beta$ subunit and small GTPases in the RGK (Rad, Rem, Rem2, and Gem/Kir) family.[31-34]

1.2 Adrenergic Regulation of $Ca_V1.2$ Via Direct Phosphorylation

A large body of evidence supports the role of PKA phosphorylation of $Ca_V1.2$ C-terminal domain (CTD), with consequent increases in channel activity, as a key component of the β-adrenergic contractile response.[23, 26, 29, 30, 35, 36] Previous work with $Ca_V1.1$ and $Ca_V1.2$ has found that the CTD is proteolytically processed, and the distal CTD associates noncovalently with the

proximal CTD and inhibits calcium conduction by the channel.[24, 25, 27] PKA phosphorylation of specific sites within the CTD relieves this potent auto-inhibition and increases $Ca_V1.2$ conductance up to 4-fold.[23]

Marked electrophysiological changes have been observed in ventricular myocytes from mice with global alanine substitutions at phosphorylation sites associated with β-adrenergic stimulation in the $Ca_V1.2$ CTD: Ser1700Ala (S1700A) and Ser1700Ala/Thr1704Ala (STAA).[28, 37, 38] In neonatal and adult cardiomyocytes from mice with global S1700A and STAA mutations, both basal and isoproterenol-stimulated calcium current were decreased by approximately ⅔ relative to WT cells.

Although these findings have been confirmed in a conditional knock-in STAA mouse model, studies using mice that expressed transgenic $Ca_V1.2$ α1-subunit with many predicted PKA phosphorylation sites in the CTD mutated to alanine nevertheless found a preserved adrenergic response.[39] Such divergent results have generated uncertainty in the field regarding the role of $Ca_V1.2$ CTD phosphorylation in β-adrenergic regulation.

Mice with global S1700A and STAA mutations also have decreased cardiac contractility, cardiac hypertrophy, and premature death at age 8-12 months.[35, 37, 38] These animals have impaired exercise capacity, increased pathological remodeling after chronic isoproterenol exposure and voluntary exercise, and lack of improvement in cardiac function after long-term β-adrenergic antagonist administration, suggesting a general loss of cardiac resilience. Interestingly, global knock-in STAA mice have been found to have a nearly preserved contractile response to high doses of β-adrenergic agonists, whereas conditional knock-in STAA animals had a substantially attenuated contractile response.[39] This suggests that long-term compensatory processes may mask the physiological role of DCT phosphorylation on adrenergic signaling.

An additional PKA phosphorylation site on the $Ca_V1.2$ CTD at position Ser1928 has been shown to have an important role in adrenergic $Ca_V1.2$ upregulation in neurons, and in mediating increased vascular reactivity in human patients with diabetes.[40, 41] Mice with global alanine substitution at position Ser1928 (S1928A) have not, however, been found to have substantial changes in baseline cardiac contractility, *in vivo* isoproterenol-induced contractile response, or Ca^{2+} current upregulation in response to high concentrations of isoproterenol.[42]

1.3 Adrenergic Regulation of $Ca_V1.2$ Via The GTPase RAD

An estimated 80% of the pore-containing α-subunit of $Ca_V1.2$ expressed in the heart is proteolytically processed at position 1800 ($Ca_V1.2\Delta1800$).[43] The proteolyzed distal C-terminal region (DCT) associates noncovalently with the channel, attenuating current conduction by the $Ca_V1.2\Delta1800$-dCT complex relative to the truncated $Ca_V1.2\Delta1800$ or the full-length channel ($Ca_V1.2$-FL).[44, 45] Activity of the autoinhibited $Ca_V1.2\Delta1800$-DCT complex can be stimulated by PKA in the presence of A-kinase anchoring proteins (AKAP).[23, 30] In heterologous expression systems and ventricular myocytes, alanine substitutions at phosphorylation sites in the $Ca_V1.2$ CTD at positions Ser1700Ala (S1700A) and Ser1700Ala/Thr1704Ala (STAA) attenuate PKA-mediated upregulation of conduction of the auto-inhibited $Ca_V1.2$ complex.[23, 28, 29, 46]

In addition to direct phosphorylation of α-subunit CTD, the binding of accessory proteins such as the Ca_V β-subunit has been observed to contribute to adrenergic upregulation of the channel.[34, 47] RAD (Ras associated with diabetes) and other members of the RGK GTPase family are more recently identified and increasingly well-characterized inhibitors of $Ca_V1.1$, $Ca_V1.2$, and $Ca_V1.3$ in myocytes and neurons.[48] RAD has been shown to bind to the α and β subunits of $Ca_V1.2$ and inhibit channel activity.[31, 33, 34, 49]

Recent work has shown that RAD inhibition of $Ca_V1.2$ can be reversed by PKA activation in a heterologous expression system, and that this effect is contingent on interactions between RAD and the $Ca_V1.2$ β-subunit, which binds to the $Ca_V1.2$ α subunit via the intracellular I-II linker.[33] Furthermore, co-expression of β-adrenergic receptors with $Ca_V1.2$ effectively reconstituted adrenergic upregulation of Ca^{2+} current in oocytes.[50] Although global RAD deletion leads to cardiac hypertrophy in mice, a recent study demonstrated that cardiac-specific RAD knockout mice had increased basal I_{Ca}, elevated ejection fraction, and no indication of concomitant pathological remodeling.[51] This study suggested that the RAD-$Ca_V1.2$ interaction may thus be considered for novel inotrope development, with the potential to avoid the induction of hypertrophy associated with currently available pro-inotropic therapeutics.

Although proteolytically processed $Ca_V1.2$ is an important form of the channel in the heart, and phosphorylation of this form is critical for adrenergic upregulation of Ca^{2+} current during the cardiac fight-or-flight response, to our knowledge no previous studies have evaluated in detail how phosphorylation of the CTD interacts with RAD in the context of the autoinhibited state.

In Chapter 3 of this work, by using heterologous co-expression of $Ca_V1.2\Delta1800$, the DCT, and RAD, we found that RAD and the DCT both inhibit $Ca_V1.2\Delta1800$, that simultaneous inhibition can be reversed by PKA stimulation, and that this reversal of inhibition is attenuated by loss of CTD phosphorylation at S1700. These observations light on the regulation of a physiologically-relevant form of $Ca_V1.2$ and RAD and show that simultaneous expression of the DCT and the GTPase can reconstitute adrenergic stimulation of the channel as co-regulators. A schematic illustrating the multiple adrenergic regulatory components of cardiac $Ca_V1.2$ is shown in Figure 1.1.

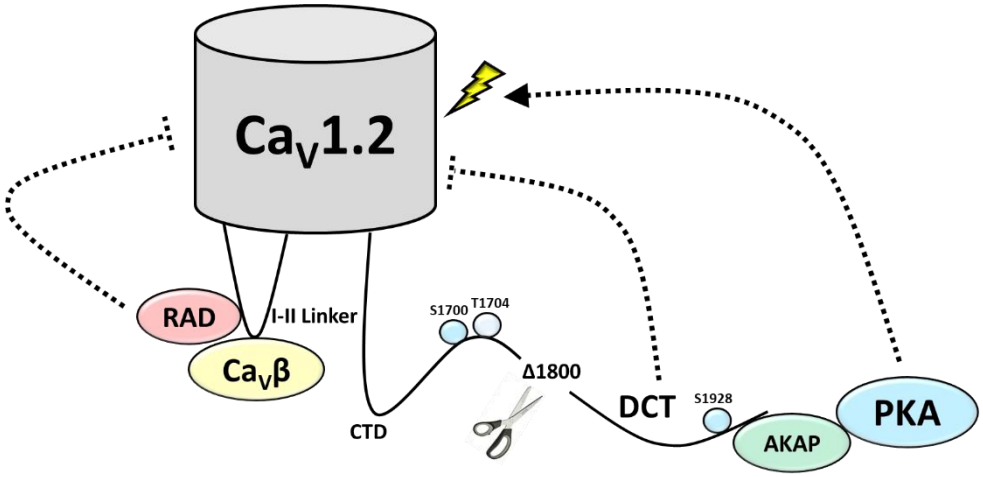

Figure 1.1. Cardiac Ca$_V$1.2 is Proteolytically Processed, Autoinhibited via its DCT, Suppressed by RAD, and Stimulated by PKA Phosphorylation

Schematic showing proteolytic processing of the CTD of the Ca$_V$1.2 α-subunit, auto-inhibition by the DCT and allo-inhibition by RAD. Also shown are phosphorylation sites at S1700, T1704, and S1928, which represent key mediators of PKA-mediated adrenergic stimulation of the channel.

1.4 Phosphoregulation of The Cardiac Ca$_V$1.2 CTD By Other Proteins

Other kinases also readily phosphorylate sites on the CTD of Ca$_V$1.2, and these proteins may have a direct or indirect role in adrenergic regulation of the channel. Mass spectrometric peptide phosphorylation studies have suggested that Ser1700 is highly phosphorylatable *in vitro* by CaMKII, as well as PKA.[23] CaMKII is a ubiquitous serine/threonine kinase, putatively bound to Ca$_V$1.2 between amino acids 1639–1660, and has been shown in numerous studies to have a critical role in driving maladaptive cardiac remodeling and CHF progression.[52-54] Two canonical CaMKII phosphorylation sites at positions S1512 and S1570 mediate the current facilitation properties of Ca$_V$1.2, although it is not clear if these phosphorylation sites impact DCT autoinhibition or channel activity regulation related to phosphorylation at S1700, T1704, and S1928. [55]

Additional β-adrenergic activation of $Ca_V1.2$ occurs via phosphorylation of Thr1704, a CK2 consensus site. CK2 is also a widely expressed serine/threonine kinase with a potential role in maladaptive remodeling.[56] Phosphorylation of this site appears to enhance the effects of phosphorylation of S1700, and its mutation to alanine in combination with the S1700A mutation results in decreased isoproterenol/forskolin stimulated Ca^{2+} currents in electrophysiological studies and more rapid progression of heart failure.[23, 28] Interestingly, transgenic overexpression of either CaMKII or CK2 leads to cardiac hypertrophy and CHF in mice, and CK2-dependent maladaptive remodeling occurs downstream of persistent angiotensin II Type I receptor activation, which is key pharmacologic target of current CHF therapies.[57]

1.5 $Ca_V1.2$ Phosphoregulation and Chronic Heart Failure

Chronic heart failure (CHF) is a leading contributor to global cardiovascular disease, with rising prevalence over the past decade.[58] CHF can be precipitated by ischemic cardiac injury, hypertension, or through the interaction of other environmental and genetic factors.[59] CHF is frequently marked by progressive maladaptive myocardial remodeling and cardiomyopathy, a process that is promoted by persistent elevation of neurohormonal stress signaling, including activation of the β-adrenergic system.[60] Pharmacologic blockade of cardiac β-adrenergic receptors is part of first-line medical therapy in established CHF, and is associated with improved survival and fewer CHF-related hospitalizations.[11]

Human clinical trials have shown that $Ca_V1.2$ antagonists lead to worse outcomes in patients with CHF, and $Ca_V1.2$ loss-of function mutations have been observed in patients with Brugada syndrome, short-QT syndrome, heart failure and sudden cardiac death.[61, 62] Human $Ca_V1.2$ gain-of-function mutations are associated with prolonged QT interval, structural cardiac defects, and neurologic disorders (Timothy syndrome). [62-65] In mice, both loss and gain-of-

function $Ca_V1.2$ mutations can induce progressive cardiomyopathy and heart failure.[35, 37-39, 66] Alanine knock-in mutations at Ser1700 (S1700A) and Ser1700/Thr1704 (STAA) cause impaired basal $Ca_V1.2$ conduction, systolic dysfunction, and slowly-progressive ventricular hypertrophy and heart failure in mice (see Fig. 1.2), whereas mutation of another $Ca_V1.2$ phosphorylation site on the C-terminal tail of the channel (Ser1928 to Ala) does not cause substantial systolic dysfunction or cardiac hypertrophy within the first year of life in mice.[29, 35, 37, 39, 42] Widely-used animal models of heart failure (left anterior artery occlusion, transverse aortic constriction, and high-dose catecholamine exposure) produce rapid pathologic remodeling and systolic impairment in a matter of days to weeks.[67] Although quickly-evolving myocardial remodeling and heart failure occur in humans under some circumstances, (e.g., Takotsubo cardiomyopathy), the most prevalent forms of human CHF are characterized by gradual disease progression and decompensation over the course of months to years.[11] The $Ca_V1.2$ S1700A and STAA phosphomutations thus generate a model of heart failure that recapitulates aspects of the progressive form of CHF often observed in human patients.

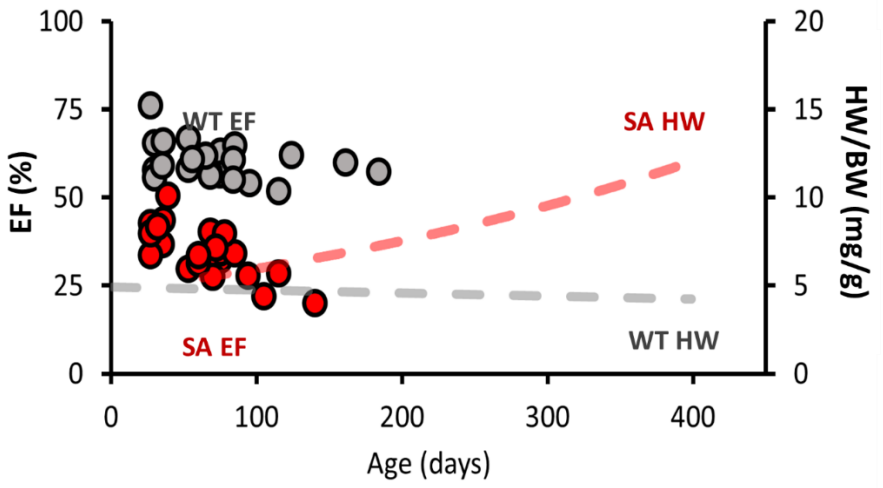

Figure 1.2. Gradual Functional Decline and Cardiac Hypertrophy in $Ca_V1.2$ Mutant Mice. Ejection fraction (EF) and mean bodyweight-normalized heart mass (HW/BW) of wildtype (WT) and $Ca_V1.2$ S1700A (SA) mice in the 1st year of life.

Chapter 2. The Role of Direct Phosphorylation of the CTD in $Ca_V1.2$ Regulation

Even as investigation into the mechanisms governing the cardiac fight-or-flight response expands to include auxiliary subunits and interacting partners of the $Ca_V1.2$ α-subunit, it is critical to understand the impact of direct phosphorylation of the α-subunit on cardiac function and fight-or-flight regulation. To evaluate the consequences of loss-of-phosphorylation mutations in the $Ca_V1.2$ CTD on *in vivo* cardiac function, we characterized the baseline cardiac functional and morphologic parameters, *in vivo* inotropic response, and the response to pressure-overload stress in mice carrying homozygous and heterozygous alanine mutations at positions S1700, STAA, and S1928 in the $Ca_V1.2$ CTD. The results of these studies describe a profound impact incurred due to phosphorylation site loss: impaired basal cardiac function, blunted response to low-dose adrenergic stimulation, and increased sensitivity to pressure overload stress. Some of these effects are even apparent in heterozygous animals, suggesting that a gene dose-dependent effect of channel phosphorylation in regulating baseline cardiac function, fight-or-flight stimulation and chronic stress resilience. This work contributes to our understanding of the functional role of $Ca_V1.2$ phosphorylation during the acute fight-or-flight response as well as persistent cardiac workload and stress.

2.1 Baseline Defects in Homozygous and Heterozygous $Ca_V1.2$ Phosphomutant Mice

$Ca_V1.2$ mutant mice with global alanine substitutions at positions Ser1700, Ser1700/Thr1704, and Ser1928 were produced as described previously.[28, 29, 42] Baseline functional and morphologic characteristics were assessed in male and female mice aged 1-4 months using

echocardiography under light isoflurane sedation. Homozygous S1700A and STAA mice showed lower baseline left-ventricular fractional shortening (FS) (Fig. 2.1A, 17.9 ± 0.8% and 18.3 ± 0.6%, respectively), compared with wildtype (WT) control animals (31.3 ± 0.6%, $p < 0.001$). Heterozygous S1700A and STAA animals also had decreased fractional shortening (26.8 ± 0.9%, $p = 0.002$; and 27.8 ± 0.6%, $p = 0.002$, respectively). Homozygous S1928A mice also had consistently reduced fractional shortening at baseline (27.1 ± 1.0%, p=0.001, which is a novel finding in contrast to a previous study showing no distinct cardiac phenotype.[42]

The homozygous S1700A and STAA showed clear evidence of ventricular hypertrophy at baseline, with increased left-ventricular end-diastolic diameter (LVEDD) (Fig. 2.1C; 4.1 ± 0.1 mm, $p = 0.0059$; and 4.22 ± 0.06 mm, $p < 0.001$, respectively) compared with WT animals (3.7 ± 0.05 mm). Interestingly, while the heterozygous S1700A (S1700A +/-), STAA (STAA +/-), and S1928A mice did not have significantly elevated LVEDD, the S1928A mice did have increased left-ventricular end-systolic diameter (LVESD) (Fig 2.1D 2.92 ± 0.097 mm, $p < 0.033$), compared with WT (2.53 ± 0.05 mm).

Baseline heart rate was significantly elevated in the S1700A and STAA mice (Table 2.1; 515 ± 6 bpm, $p < 0.001$; and 504 ± 7 bpm, $p < 0.001$) compared with WT (466 ± 7 bpm), but was not elevated in the heterozygous animals. Homozygous S1928A animals had depressed heart rate compared with WT animals (410 ± 8 bpm, $p < 0.001$). Heart weight was higher in mice with homozygous S1700A and STAA mutations (Table 1; 6.2 ± 0.1 mg/g bodyweight, $p = 0.059$; and 6.6 ± 0.2 mg/g, $p = 0.037$, respectively), compared with WT animals (4.7 ± 0.2 mg/g). These findings are consistent with previous evidence of hypertrophy and CHF in these mice.

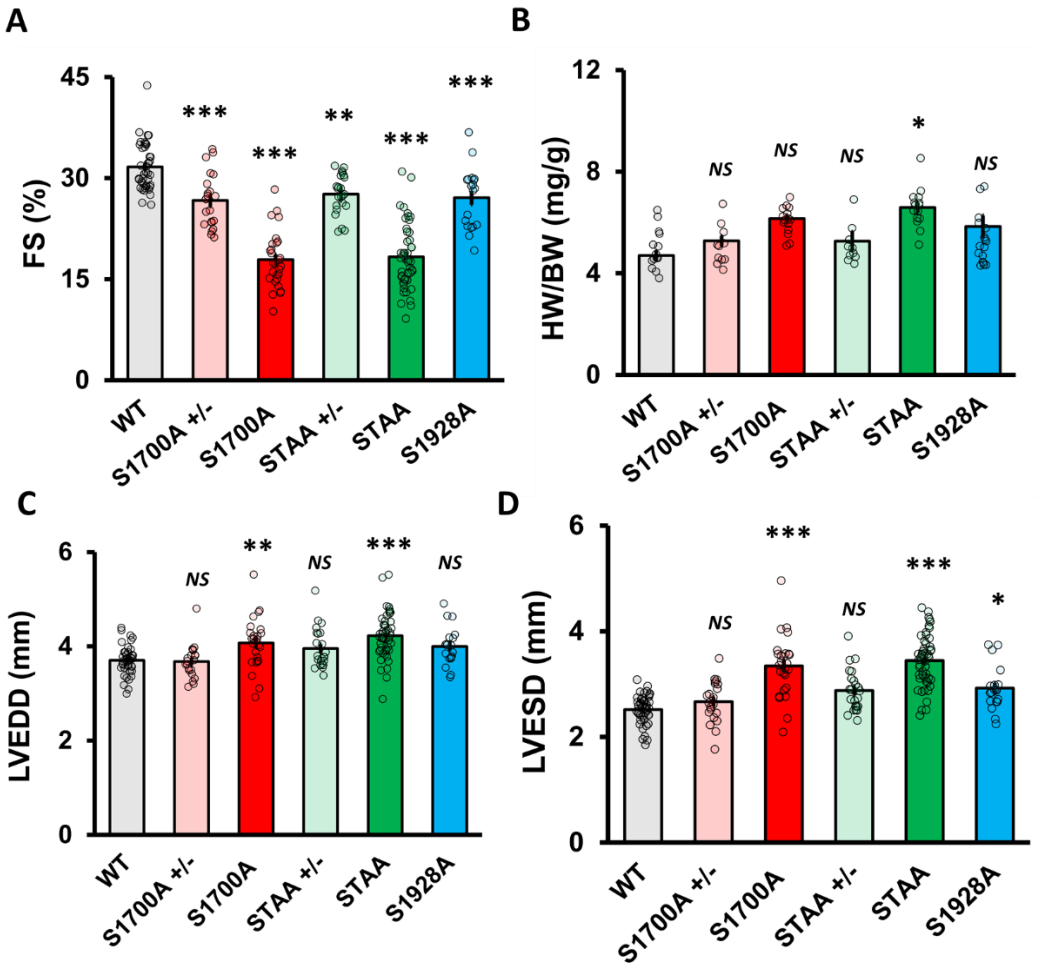

Figure 2.1. Impaired Baseline Systolic Function in Mice with Heterozygous and Homozygous Cav1.2 Phosphoregulatory Site Mutations

Left-ventricular (A) fractional shortening, (B) bodyweight normalized cardiac mass, (C) end-diastolic diameter and (D) end-systolic diameter in young WT, heterozygous and homozygous S1700A and STAA mice, and homozygous S1928A mice. Statistical significance determined via ANOVA and post-hoc Tukey HSD comparison to WT. Error bars are S.E.M.; N =- 41 (WT), 28 (S1700A), 53 (STAA), 19 (S1928A), 23 (STAA +/-), 21 (S1700A +/-); * $p < 0.05$, ** $p < 0.01$, *** $p < 0.001$.

2.2 In Vivo Inotropic Response to β-Adrenergic Stimulation

Earlier literature primarily describes the administration of supraphysiologic doses of β-adrenergic agonists to mice with mutations in $Ca_V1.2$ phosphoregulatory sites, often exceeding 100 μg of drug per kg bodyweight. To investigate the impact of phosphoregulatory $Ca_V1.2$ mutations on cardiac adrenergic regulation at more physiological levels of catecholamine, we performed a dose-ranging study to evaluate the *in vivo* inotropic response at a range of doses of isoproterenol (Fig. 2.2A, B). Three doses of isoproterenol were intraperitoneally administered to mice aged 5-15 weeks. The low-dose group received 0.25 μg/kg, the intermediate group received 1 μg/kg, and the high-dose group received 100 μg/kg of isoproterenol.

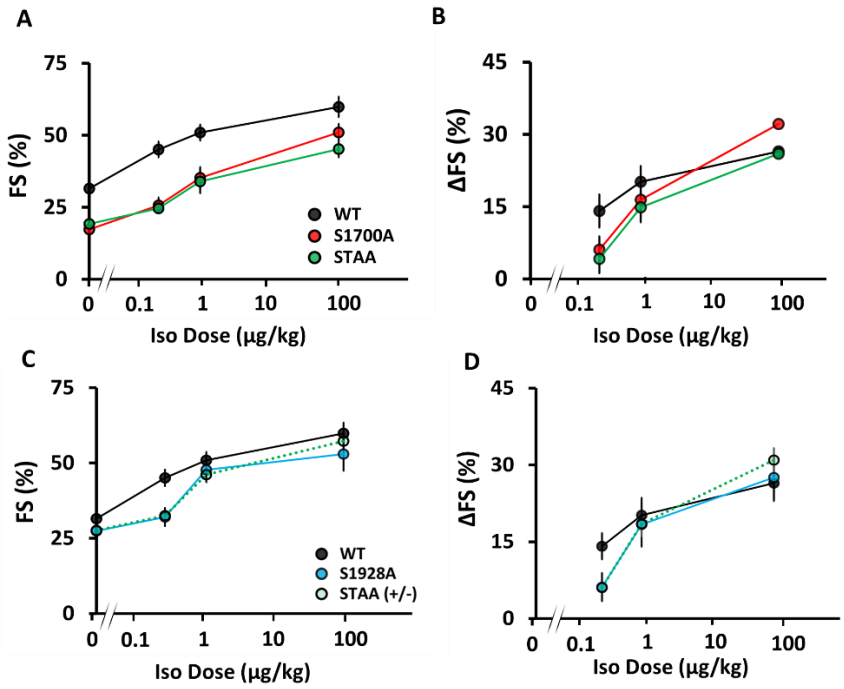

Figure 2.2. Inotropic Dose-Response to β-Adrenergic Stimulation in Mice with $Ca_V1.2$ Phosphoregulatory Site Mutations

Isoproterenol dose-response assessed via (A) fractional shortening and (B) change in fractional shortening in WT, S1700A, STAA mice, and (C) fractional shortening and (B) change in fractional shortening in WT, STAA +/-, and and S1928A mice, in response to intraperitoneal

drug administration. Statistical significance determined via ANOVA with Tukey post-hoc tests. Error bars are S.E.M.; $N_{0.25\ \mu g/kg}$ =- 9, 8, 6, 8, 8 (for WT, S1700A, STAA, S1928A, STAA +/-, respectively); $N_{1\ \mu g/kg}$ =- 6, 7, 8, 6, 9 (for WT, S1700A, STAA, S1928A, STAA +/-, respectively); $N_{100\ \mu g/kg}$ =- 7, 7, 7, 7, 11 (for WT, S1700A, STAA, S1928A, STAA +/-, respectively); * $p< 0.05$, ** $p< 0.01$, *** $p < 0.001$.

To investigate the impact of phosphoregulatory $Ca_V1.2$ mutations on cardiac adrenergic regulation at physiological levels of β-adrenergic stimulation, we compared the *in vivo* inotropic responses of mice at two physiologic doses (0.25 μg/kg and 1 μg/kg) and one supraphysiologic dose (100 μg/kg) of isoproterenol (Fig. 2A, B). In the S1700A and STAA mice, baseline FS in the absence of isoproterenol was significantly reduced relative to controls (WT, 31.3 ± 0.6%; STAA, 17.9 ± 0.8%; S1700A 18.3 ± 0.6%; Fig. 2.2A). Treatment with 0.25 μg/kg isoproterenol produced a smaller increment in FS for STAA and S1700A than observed in the WT mice (Fig. 2A). This difference is seen more clearly in Fig. 2B where the increment in FS caused by isoproterenol (ΔFS) is plotted vs. isoproterenol dose (6 ± 1%, $p = 0.048$ and 4 ± 1%, $p = 0.018$ respectively) compared with WT (14 ± 3%). The stimulated FS values of these mice were still markedly depressed compared with stimulated WT animals at the intermediate 1 μg/kg dose (Fig. 2.2A, B: S1700A, 26 ± 3%, $p < 0.001$; STAA, 25 ± 1%, $p < 0.001$; WT, 45 ± 3%). On the other hand, administration of the highest dose of isoproterenol (100 μg/kg), produced larger FS (Fig. 2.2A) and larger ΔFS (Fig. 2.2B: S1700A, 32 ± 4%; $p = 0.79$; STAA, 26 ± 3%; $p = 1.0$), which were comparable to WT (26 ± 3%). These results show that the β-adrenergic response is impaired by these phoshoregulatory site mutations in $Ca_V1.2$ at physiological doses of isoproterenol, whereas higher doses are able to overcome the deficit in β-adrenergic signaling caused by the phosphoregulatory mutations.

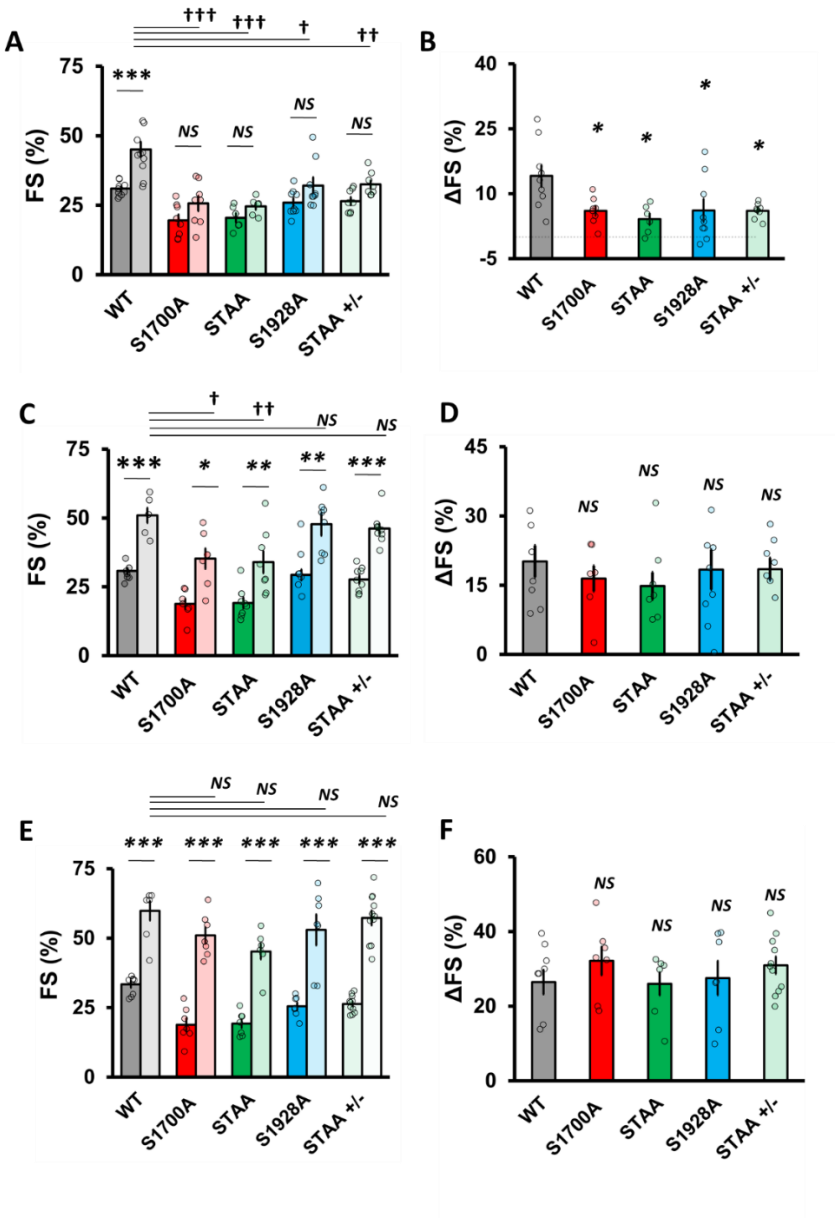

Figure 2.3. Impaired Inotropic Response to Physiologic Range β-Adrenergic Stimulation in Mice with Cav1.2 Phosphoregulatory Site Mutations

(A) Fractional shortening and (B) change in fractional shortening in WT, S1700A, STAA, and S1928A, and STAA heterozygous (+/-) mice before and after 0.25 μg/kg intraperitoneal isoproterenol administration. (C) Fractional shortening and (D) change in fractional shortening intraperitoneal before and after 1 μg/kg drug administration. (E) Fractional shortening and (F)

change in fractional shortening intraperitoneal before and after 100 μg/kg drug administration. Statistical significance determined via ANOVA with Tukey post-hoc tests Error bars are S.E.M.; $N_{0.25\ \mu g/kg}$ =- 9, 8, 6, 8, 8 (for WT, S1700A, STAA, S1928A, STAA +/-, respectively); $N_{1\ \mu g/kg}$ =- 6, 7, 8, 6, 9 (for WT, S1700A, STAA, S1928A, STAA +/-, respectively); $N_{100\ \mu g/kg}$ =- 7, 7, 7, 7, 11 (for WT, S1700A, STAA, S1928A, STAA +/-, respectively). $p< 0.05$, ** $p< 0.01$, *** $p < 0.001$ for comparisons against baseline, † $p< 0.05$, †† $p< 0.01$, ††† $p < 0.001$ for comparisons against stimulated WT.

The inotropic responses to the different doses of isoproterenol and their statistical significance are illustrated in more detail in Fig. 2.3. At the lowest dose (0.25 μg/kg), WT mice showed a statistically significant increase in FS, whereas S1700A and STAA mutant mice did not (Fig. 3A), and these mutant mice had significantly reduced ΔFS compared to WT (Fig. 2.3B). At the intermediate dose of 100 μg/kg, both strains of mutant mice showed a significant increase in FS with isoproterenol treatment (Fig. 2.3C), and their ΔFS in response to isoproterenol was not significantly reduced compared to WT (Fig. 2.3D). At the highest dose (100 μg/kg), S1700A and STAA mutant mice had similar responses in both FS and ΔFS to WT mice.

Longstanding impairment in contractility can lead to β-adrenergic desensitization through mechanisms that are unrelated to $Ca_V1.2$ phosphoregulation. Therefore, we also evaluated the impact of the heterozygous STAA mutation and the homozygous S1928A mutation on the β-adrenergic inotropic response because these mice have only mildly decreased contractility at baseline and do not develop heart failure. As with the homozygous S1700A and STAA animals, these heterozygous mice exhibited a deficit in their response to low-dose isoproterenol stimulation of FS (Fig. 2.2C, D and Fig. 2.3A, B: stimulated FS, S1928A, 34 ± 2%, $p = 0.015$; STAA +/-, 33 ± 2%, $p =0.008$) compared with WT (45 ± 3%). Unlike the S1700A and homozygous animals, S1928A and STAA +/- animals responded normally to the intermediate dose of isoproterenol,

achieving FS comparable to WT (Fig. 3C, D. S1700A: 35 ± 4%; p = 0.021; STAA: 34 ± 4%; p = 0.008; S1928A: 48± 4%; p = 0.97; STAA +/-: 46 ± 4%; p = 0.83; WT: 51 ± 3%). As for homozygous mutant S1700A and STAA mice, heterozygous STAA mice homozygous S1928A mice exhibited responses to the highest dose of isoproterenol that were indistinguishable from WT (Fig. 2.2C, D; Fig. 2.3E, F).

These findings indicate that the contractility of S1928A and STAA +/- diverges from WT contractility at baseline and at our lowest dose of isoproterenol, but these mutants achieve levels of function commensurate with WT at intermediate and high doses. In contrast, the S1700A and STAA mice have defective responses to the low and intermediate doses of isoproterenol and require very high doses to achieve stimulated contractile function similar WT controls. For these mice, physiological levels of β-adrenergic inotropic response can be completely achieved only at supramaximal levels of hormonal activation.

2.3 Exacerbated Remodeling in Homozygous S1700A and STAA Mice After Aortic Constriction

Our previous results showed that S1700A and STAA mice develop severe hypertrophy and lethal CHF as they age over 100 days. However, these mice are healthy at younger ages. We tested whether reduced β-adrenergic regulation caused by mutation of phoshoregulatory sites on $Ca_V1.2$ channels would be beneficial in pressure-induced CHF or would exacerbate this pathological condition. After baseline echocardiography, heterozygous and homozygous SA and STAA mice aged 50-90 days underwent transverse aortic constriction (TAC) surgery to induce persistent cardiac pressure-overload stress. Cardiac function and morphology were assessed weekly and animals were euthanized four weeks after the surgery (Fig. 2.4A-C).

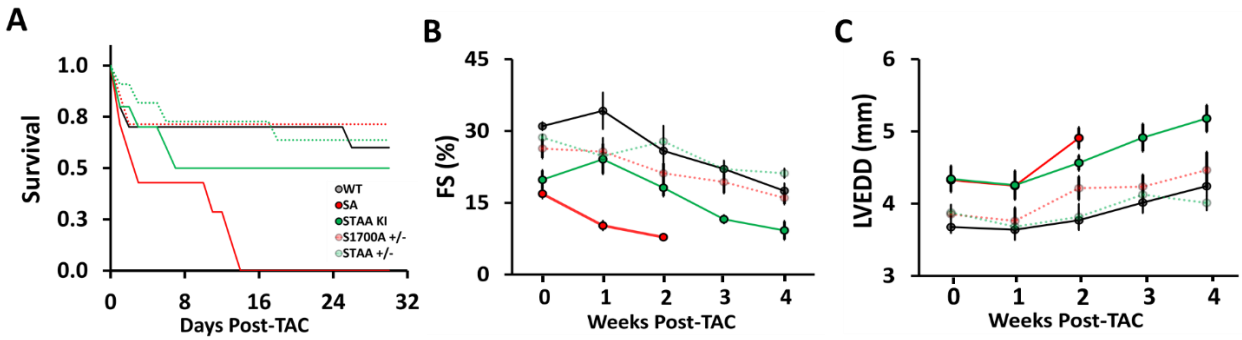

Figure 2.4. Exacerbation of Pressure-Induced Heart Failure and Premature Death Following Homozygous Mutation of Cav1.2 Phosphoregulatory Sites

(A) Survival rates after TAC for WT (gray markers), heterozygous SA (light red) and STAA (light green), and homozygous SA (red) and STAA (green) mice aged 50-90 days. Left-ventricular (B) fractional shortening and (C) end-diastolic diameter measured at 1 week intervals following TAC surgery. Error bars are S.E.M.; $N_{4\ Weeks}$ =- 6 (WT), 5 (STAA), 7 (STAA +/-), 5 (S1700A +/-). * $p < 0.05$, ** $p < 0.01$, *** $p < 0.001$.

S1700A and STAA mice had lower survival rates than WT following TAC (Fig. 2.4A). Surprisingly, homozygous mice with only the S1700A mutation experienced a significantly lower postsurgical survival rate compared with STAA mice, with no surviving animals by 4 weeks post-surgery. Due to the high mortality in the S1700A mice, we discontinued further surgeries on this line. Half of the STAA animals that underwent surgery survived until 4 weeks, compared with 60-70% of the WT and heterozygous mice (Fig. 4A).

Four weeks after surgery, surviving STAA mice had notably decreased fractional shortening (Fig. 2.4B, Fig. 5A: 9 ± 2%, p = <0.001) compared with WT animals (18 ± 2%), albeit with a comparable absolute loss of contractility measured as FS (Fig. 2.5B: ΔFS STAA, -15 ± 2; WT:,-13 ± 1, p = 0.82). However, STAA mice showed marked signs of accelerated cardiac remodeling compared with controls. We observed a significant increase in ventricular dilation in STAA mice (Fig. 2.4C/5C: LVEDD, STAA pre-TAC, 4.07 ± 0.09 mm vs post-TAC, 5.2 ± 0.1; p

< 0.001), whereas WT mice experienced a less severe increase in ventricular volume (Fig.5C: WT, pre-TAC, 3.7 ± 0.1 mm vs post-TAC, 4.2 ± 0.1, p = 0.081). HW/BW also increased more in STAA mice than in WT mice when compared to animals that did not receive TAC (Fig. 2.5D: STAA, no-TAC, 6.6 ± 0.2 mg/g vs post-TAC, 8.4 ± 0.3; p < 0.047; WT no-TAC 4.7 ± 0.2 mg/g vs post-TAC: 5.9 ± 0.5; p = 0.42).

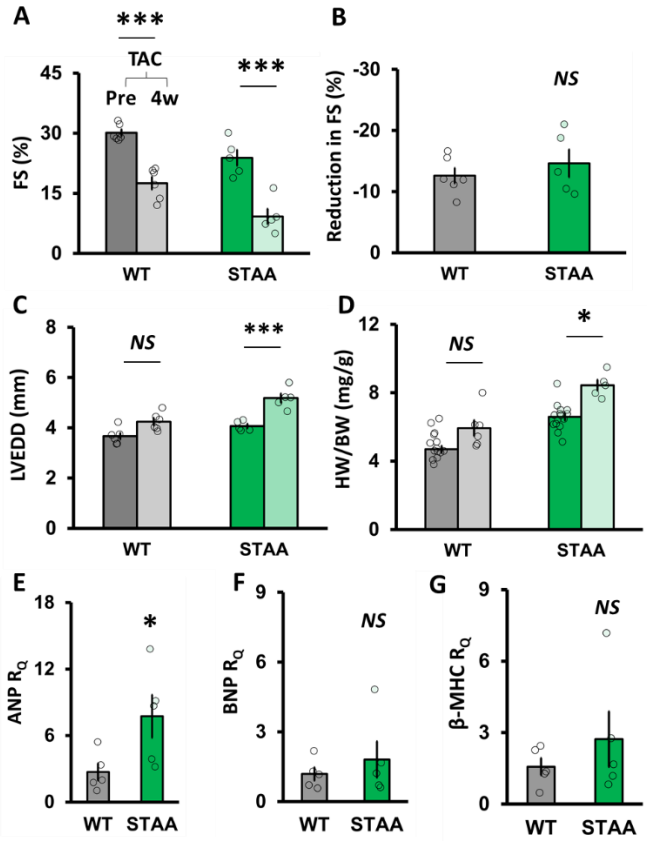

Figure 2.5. Hypertrophy and Ventricular Dilation After TAC in Mice with Homozygous Mutations of $Ca_V1.2$ Phosphoregulatory Sites

(A) Fractional shortening, (B) reduction fractional shortening, (C) left-ventricular end-diastolic diameter, and (D) body-weight normalized heart-weight 4 weeks after TAC surgery (right bars) and in non-TAC control animals (left bars) in WT and homozygous STAA mice. (E-F) Expression fold-change in ANP, BNP, and β-MHC hypertrophic markers in ventricular tissue of WT and homozygous STAA mice after TAC relative to age-matched control animals. Statistical

significance determined via ANOVA with Tukey post-hoc tests Error bars are S.E.M.; $N_{4\ Weeks}$ =-6 (WT), 5 (STAA); $N_{NoTacControls}$ = 13 (WT), 14 (STAA). * $p < 0.05$, ** $p < 0.01$, *** $p < 0.001$.

Expression of hypertrophic markers was elevated in both WT and STAA mice post-TAC, compared with age-matched control animals without TAC, with greater relative quantification (R_Q) values of atrial natriuretic peptide (ANP) mRNA in the STAA animals (Fig. 2.5E; RQ ANP: STAA, 7.74 ± 1.94 vs WT, 2.72 ± 0.41; $p = 0.039$). BNP and β-MHC were comparably elevated in both WT and STAA post-TAC animals (Fig. 2.5F/G).

2.4 Minor Changes in Heterozygous S1700A and STAA Mice After Aortic Constriction

Unlike homozygous S1700A and STAA animals, young heterozygous S1700A and STAA animals tolerated TAC well, and experienced comparable changes in FS, HW/BW, LVEDD, and hypertrophic markers as WT animals. In fact, the STAA +/- cohort exhibited a trend towards less attenuated loss of contractility compared with WT animals (Fig 2.6B: ΔFS, STAA +/-, -7 ± 1%, $p = 0.12$; S1700A +/-, - 7 ± 2%, $p = 0.16$; WT, -13 ± 1%).

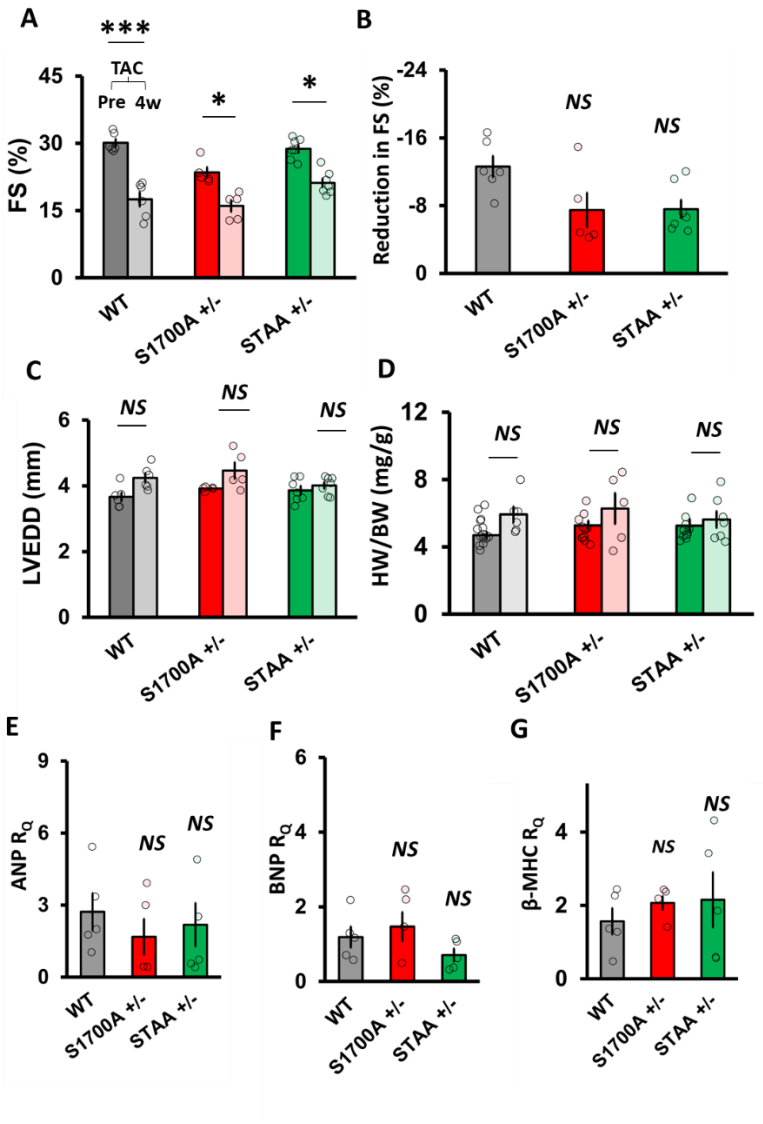

Figure 2.6. Attenuated Ventricular Changes After TAC in Mice with Heterozygous Mutations of Cav1.2 Phosphoregulatory Sites

(A) Fractional shortening, (B) reduction in fractional shortening, (C) left-ventricular end-diastolic diameter, and (D) body-weight normalized heart-weight 4 weeks after TAC surgery (right bars) and in non-TAC control animals (left bars) in WT, heterozygous S1700A, and heterozygous STAA mice. (E-F) Expression fold-change in ANP, BNP, and β-MHC hypertrophic markers in ventricular tissue of WT and homozygous STAA mice after TAC relative to age-matched control animals. Statistical significance determined via ANOVA with Tukey post-hoc tests. Error bars are S.E.M.; $N_{4\ Weeks}$ =- 6 (WT), 7 (STAA +/-), 5 (S1700A +/-); $N_{NoTacControls}$ = 13 (WT), 9 (STAA +/-), 9 (STAA +/-). * $p < 0.05$, ** $p < 0.01$, *** $p < 0.001$.

Table 2.1. Baseline and Isoproterenol-Stimulated Cardiac Parameters in Mice with $Ca_V1.2$ Phosphoregulatory Site Mutations

	WT	S1700A	STAA	S1928A	STAA (+/-)	S1700A (+/-)
Baseline						
FS ± SEM (%)	31.7 ± 0.6	17.9 ± 0.8	18.3 ± 0.6	27 ± 1	27.6 ± 0.6	26.7 ± 0.9
p-value FS vs WT	N = 41	<0.001; N = 28	<0.001 ; N = 53	0.003; N = 19	0.016; N = 23	<0.001 ; N = 21
HR ± SEM (BPM)	468 ± 7	515 ± 6	504 ± 7	410 ± 8	468 ± 9	486 ± 9
p-value HR vs WT		<0.001	<0.001	<0.001	1.00	0.36
LVEDD ± SEM (mm)	3.70 ± 0.05	4.1 ± 0.1	4.22 ± 0.06	4.00 ± 0.09	3.96 ± 0.09	3.68 ± 0.08
p-value LVEDD vs WT		0.0059	<0.001	0.099	0.29	1.00
LVESD ± SEM (mm)	2.52 ± 0.04	3.3 ± 0.1	3.44 ± 0.07	2.9 ± 0.1	2.88 ± 0.08	2.67 ± 0.09
p-value LVEDD vs WT	N = 41	<0.001	<0.001	0.033	0.070	0.87
HW/BW ± SEM (mg/g)	4.7 ± 0.2	6.2 ± 0.1	6.6 ± 0.2	5.8 ± 0.4	5.3 ± 0.4	5.3 ± 0.3
p-value HW/BW vs WT	N = 10	0.059; N = 14	0.037; N = 15	0.46; N = 19	0.84; N = 18	0.92; N = 8
0.25 µg/kg Cohort						
$FS_{Baseline}$ ± SEM (%)	31.0 ± 0.9	20 ± 2	20 ± 2	26 ± 2	26 ± 1	
$FS_{Iso,\ 0.25\ µg/kg}$ ± SEM (%)	45 ± 3	26 ± 3	25 ± 1	32.1 ± 3	32 ± 1	
p-value FS_{Iso} vs Baseline	<0.001 ; N = 9	0.69; N =8	0.98; N = 6	0.040; N = 8	0.76; N = 8	
p-value FS_{Iso} vs WT FSi_{so}		<0.001	<0.001	0.015	0.0081	
ΔFS ± SEM (%)	14 ± 3	6 ± 1	4 ± 1	6 ± 3	6 ± 1	
p-value ΔFS vs WT		0.048	0.018	0.042	0.048	
1 µg/kg Cohort						
$FS_{Baseline}$ ± SEM (%)	31 ± 1	19 ± 2	19 ± 2	29 ± 2	28 ± 1	
$FS_{Iso,\ 1\ µg/kg}$ ± SEM (%)	51 ± 3	35 ± 4	34 ± 4	48 ± 4	46 ± 2	
p-value; FS_{Iso} vs Baseline	<0.001; N = 6	0.039; N = 7	0.0074 ; N = 8	0.0023; N = 6	<0.001 ; N = 9	
p-value FS_{Iso} vs WT FSi_{so}		0.021	0.0084	0.97	0.83	
ΔFS ± SEM (%)	20 ± 3	16 ± 3	15 ± 3	18 ± 4	18 ± 2	
p-value ΔFS vs WT		0.93	0.83	0.99	1.0	
100 µg/kg Cohort						
$FS_{Baseline}$ ± SEM (%)	33 ± 1	19 ± 2	19 ± 2	25 ± 1	26.3 ± 0.9	
$FS_{Iso,\ 100\ µg/kg}$ ± SEM (%)	60 ± 4	51 ± 3	45 ± 3	53 ± 6	57 ± 3	
p- value FS_{Iso} vs Baseline	<0.001; N = 7	<0.001; N = 7	<0.001; N = 7	<0.001; N = 7	<0.001; N = 11	
p-value FS_{Iso} vs WT FSi_{so}		0.61	0.12	0.82	1	
ΔFS ± SEM (%)	26 ± 3	32 ± 4	26 ± 3	28 ± 5	31 ± 2	
p-value ΔFS vs WT		0.79	1.0	1.0	0.90	

2.5 Impaired Baseline Contractility and Pathological Hypertrophy in S1700A, STAA, and S1928A Mice

As reported previously, young adult homozygous S1700A mice have systolic dysfunction and significant ventricular remodeling, which is also observed in our cohort of S1700A mice studied here.[38] Extending this previous work, we found here that animals with homozygous STAA mutations also have substantially impaired cardiac performance, pathological hypertrophy, and heart failure, which is consistent with previous work with a different mouse line analogous to STAA mice.[39]

In contrast to homozygous mutants, mice with heterozygous S1700A and STAA mutations have a less marked depression of contractile function that is not sufficient to cause significant hypertrophy or ventricular dilation. This suggests that partial loss of phosphorylation of $Ca_V1.2$ in heterozygous mutants is tolerable, producing mild changes in basal contractility without hypertrophic changes.

Earlier work characterizing homozygous $Ca_V1.2$ S1928A mice described no major adverse cardiac phenotype.[42] In this study, we found an absolute reduction of 7% (4.6% ΔFS) in baseline ejection fraction compared with wild-type animals, without indication of cardiac hypertrophy or dilation. This suggests that S1928 phosphorylation may contribute to regulation of basal cardiac contractility, but its loss does not lead to progressive dysfunction and heart failure.

These *in vivo* basal contractility findings in heterozygous S1700A and T1704A mice and in homozygous S1928A mice provide further evidence for the functional role of protein kinase regulation of basal $Ca_V1.2$ channel activity through phosphorylation of the C-terminal region at sites S1700, T1704, and S1928. It appears that animals with long-term heterozygous loss of S1700A, T1704, and homozygous loss S1928 phosphorylation are able to compensate and retain

a normal range of cardiac function, whereas homozygous mutations S1700A and STAA lead to severe systolic dysfunction, hypertrophy, and premature death. Previous studies showed that the density and localization of $Ca_V1.2$ channel protein were not significantly altered in the S1700A or STAA mice in C57BL/6J genetic background studied here.[37] Therefore, these deficits in cardiac function at baseline in vivo are consistent with previous conclusions that phosphorylation of Ser1700 and Thr1704 is important for maintenance of basal calcium current conducted by $Ca_V1.2$ channels and for basal contractile function in ventricular myocytes. Moreover, we find that the homozygous mutation S1928A also significantly impairs cardiac function *in vivo*, supporting a three-site regulatory mechanism for basal $Ca_V1.2$ function by protein phosphorylation of the C-terminal domain.

Table 2.2. TAC Response in Mice with Cav1.2 Phosphoregulatory Site Mutations

	WT	STAA	S1700A	STAA (+/-)	S1700A (+/-)
$FS_{Baseline}$ ± SEM (%)	30.1 ± 0.8	23.9 ± 2	16.9 ± 0.9	28.8 ± 0.9	24 ± 1
FS_{4W} ± SEM (%)	18 ± 2	9 ± 2		21 ± 1	16 ± 1
p-value FS_{4W} vs $FS_{Baseline}$	<0.001; N = 6	<0.001; N = 5		0.013; N = 7	0.016; N = 5
ΔFS ± SEM (%)	-13 ± 1	-15 ± 2		-8 ± 1	-7 ± 2
p-value ΔFS vs WT		0.82		0.12	0.16
$LVEDD_{Baseline}$ ± SEM (mm)	3.7 ± 0.1	4.07 ± 0.09	4.3 ± 0.1	3.9 ± 0.1	3.92 ± 0.03
$LVEDD_{4W}$ ± SEM (mm)	4.2 ± 0.1	5.2 ± 0.2		4.0 ± 0.1	4.5 ± 0.2
p-value $LVEDD_{4W}$ vs $LVEDD_{Baseline}$	0.081	<0.001		0.99	0.093
HW/BW_{4W} ± SEM (mg/g)	5.9 ± 0.5	8.4 ± 0.3		5.6 ± 0.5	6.3 ± 0.9
p-value HW/BW_{4W} vs No TAC	0.42	0.047		1.0	0.79
# Animals Receiving TAC	N = 10	N = 10	N = 7	N = 11	N = 10
# Animals Alive 4 Weeks Post-TAC	N = 6	N = 5	N = 0	N = 7	N = 5
ANP					
$\Delta C_{T,\ No\ TAC}$ ± SEM	6.5 ± 0.6; N = 13	5.8 ± 0.8; N = 14		3.2 ± 0.3; N = 9	3.3 ± 0.4; N = 9
$\Delta C_{T,\ TAC}$ ± SEM	5.3 ± 0.4; N = 5	3.0 ± 0.4; N = 5		3.0 ± 0.7; N = 5	3.2 ± 0.7; N = 5
$R_Q\ [2^{-(\Delta C_{T,TAC} - \Delta C_{T,NoTAC})}]$ ± SEM	2.7 ± 0.4	8 ± 2		2.2 ± 0.9	1.7 ± 0.7
p-value R_Q vs WT		0.039		1.0	0.90
BNP					
$\Delta C_{T,\ No\ TAC}$ ± SEM	6.3 ± 0.4 (N = 14)	5.2 ± 0.5 (N = 14)		4.8 ± 0.3 (N = 9)	5.4 ± 0.3 (N = 9)
$\Delta C_{T,\ TAC}$ ± SEM	6.2 ± 0.34 (N = 5)	4.8 ± 0.5 (N = 5)		5.5 ± 0.4 (N = 5)	5.1 ± 0.5 (N = 5)
$R_Q\ [2^{-(\Delta CT,TAC - \Delta CT,NoTAC)}]$ ± SEM	1.2 ± 0.3	1.8 ± 0.8		0.7 ± 0.2	1.5 ± 0.4
p-value R_Q vs WT		0.78		0.86	0.90
β-*MHC*					
$\Delta C_{T,\ No\ TAC}$ ± SEM (*N*)	7.0 ± 0.5 (N = 13)	5.9 ± 0.4 (N = 14)		7.6 ± 0.4 (N = 8)	7.2 ± 0.6 (N = 9)
$\Delta C_{T,\ TAC}$ ± SEM (*N*)	6.6 ± 0.4 (N = 5)	4.9 ± 0.5 (N = 5)		6.9 ± 0.6 (N = 5)	6.2 ± 0.1 (N = 5)
$R_Q\ [2^{-(\Delta CT,TAC - \Delta CT,NoTAC)}]$ ± SEM	1.6 ± 0.4	3 ± 1		2.2 ± 0.8	2.1 ± 0.2
p-value R_Q vs WT		0.66		1.0	0.90

2.6 Reduced Response to Physiological β-Adrenergic Stimulation in S1700A, STAA, and S1928A Mice

In vivo studies of β-adrenergic regulation of cardiovascular function in mice with $Ca_V1.2$ mutations has typically been performed at very high doses of isoproterenol ($\geq$ 100 μg/kg bodyweight), well beyond the estimated range of adrenergic stimulation *in vivo*.[42, 68] Elevated doses of isoproterenol may produce non-physiological responses and could mask physiologically relevant effects of mutations on $Ca_V1.2$ channels on the heart. The current study therefore investigated the dose-response of homozygous S1700A, STAA, and S1928A mice at a range of concentrations of isoproterenol (0.25 - 100 μg/kg bodyweight) that mimic the range of physiological stimulation in vivo.

Notably, we found that the lowest dose of isoproterenol (0.25 μg/kg) evokes a 13% absolute increase in fractional shortening in WT mice, but approximately half of that response was observed in S1700A, STAA, S1928A, and STAA +/- mice. Therefore, at low doses of isoproterenol, the β-adrenergic response is likely impaired by mutations in all three of these C-terminal phosphorylation sites and is unable to mediate a contractile stimulation as robust as a WT animal. The attenuated isoproterenol response of the S1700A and STAA mice could be mediated in part by maladaptive compensatory processes, such as β-adrenergic receptor desensitization due to persistently depressed contractility, even in the young mice studied here. However, this is less plausible in the S1928A and STAA +/- mice, which have only mildly impaired ejection fraction and do not develop hypertrophy and heart failure. It is thus possible that the contribution of S1928A to the acute cardiac adrenergic response has been previously overlooked due to use of non-physiological doses of β-adrenergic agonist. Although the role of S1928 still appears to be less critical for the cardiac adrenergic response than for the neuronal or smooth muscle

upregulation of $Ca_V1.2$ activity, our findings suggest it may have a role in regulating basal contractility and supporting the fight-or-flight response in the context of physiological levels of catecholamine stimulation.

At intermediate (1 μg/kg) and high doses (100 μ/kg) of isoproterenol, all four genotypes (WT, S1700A, STAA, S1928A) of mice reached ejection fractions of nearly 90% (FS 50%). This preserved adrenergic reserve may be the result of long-term compensatory processes, as earlier work has shown that compensatory processes enhance contractility measured at the single-cell level and shorter-term conditional knock-in mutant of the STAA sites in a different genetic background does not have a robust adrenergic response.[32, 39, 69] Overall, by using a range of doses of isoproterenol that produce physiologically relevant stimulation *in vivo*, our studies show that the S1700A and STAA mutations cause a substantial reduction in the β-adrenergic increase in cardiac contractility, whereas the S1928A mutation has smaller, but still significant effects.

2.7 Interaction of S1700A and STAA Mutations with Pressure Overload Stress

To further evaluate the effect of the S1700A and STAA mutations on cardiac resilience and the development of heart failure, we investigated the effect of chronic pressure overload on heterozygous and homozygous S1700A and STAA mice. Previous work has shown that in WT mice, β-adrenergic blockade is effective at mitigating the consequences of TAC on cardiac hypertrophy.[70] We thus hypothesized that mice with either heterozygous or homozygous mutations at PKA phosphorylation sites on $Ca_V1.2$, which serve as putative downstream mediators of β-adrenergic signaling, might be protected against pathologic remodeling due to pressure overload.

We found, however, that mice with homozygous S1700A mutations had markedly lower survival rate 4 weeks after TAC compared with WT animals. Although the STAA homozygous

mice had a better survival rate than the S1700A mice, they also developed severely decreased ejection fractions and accelerated signs of cardiac hypertrophy compared with wild-type and heterozygous animals.

On the other hand, heterozygous S1700A and STAA mice had similar responses to WT mice after TAC surgery, with comparable losses in ejection fraction and hypertrophic changes. This indicates that the heterozygous loss of phosphorylation at these sites - despite producing a mild reduction in contractility at baseline - does not substantially impair the ability of the mice to compensate for chronic pressure overload stress. These findings provide additional evidence for the tolerability of partial, but not total, loss of PKA phosphorylation at S1700 and T1704 on the $Ca_V1.2$ DCT.

This gene dose-dependent tolerability of loss of S1700 and T1704 phosphorylation may also shed light on the unexpected findings in mice expressing transgenic $Ca_V1.2$ with loss of all PKA phosphorylation on the DCT.[32, 69] In those studies, endogenous wild-type $Ca_V1.2$ is blocked with a dihydropyridine, permitting measurement of transgenic, non-phosphorylatable dihydropyridine-insensitive $Ca_V1.2$ current. It is possible that preserved PKA phosphorylation at incompletely blocked, endogenous, non-transgenic channels may be sufficient to generate a preserved adrenergic response in response to non-physiological high doses of isoproterenol because of the reserved capacity that we have observed in Ser1700A and Thr1704A mice here.

2.8 Conclusions

In this study we report that the $Ca_V1.2$ S1700A, STAA, and S1928A mutations impact basal cardiac contractility and alter cardiac morphology in young mice. These mutations also blunt the isoproterenol response at low, physiologic-range doses. Finally, the homozygous S1700A and STAA mutations worsen post-TAC survival and hypertrophy. Together, these results show that

phosphorylation of key PKA sites on the CTD of $Ca_V1.2$ has an essential role in basal regulation of contractility, β-adrenergic inotropic responses to physiological levels of stimulation, and compensation for pressure-overload stress.

Chapter 3. Adrenergic Regulation of $Ca_V1.2$ by the GTPase RAD

The small GTP-binding protein RAD (Ras associated with diabetes) has emerged as a potent regulator of $Ca_V1.2$, conferring robust channel inhibition that is relieved by PKA stimulation.[33, 34, 50, 51] It is not yet known how RAD regulation interacts with DCT inhibition and direct phosphorylation of the $Ca_V1.2$ α subunit, and whether these mechanisms are redundant, complementary, or synergistic in the regulation of excitation-contraction coupling. Here, I used electrophysiological methods to determine the relationship between $Ca_V1.2$ inhibition by RAD and the $Ca_V1.2$ distal C-terminus (DCT), and elucidate the role of PKA-mediated phosphorylation in relieving channel inhibition by these respective entities. Using heterologous co-expression of $Ca_V1.2\Delta1800$, the DCT, and RAD, I found that RAD and the DCT both inhibit $Ca_V1.2\Delta1800$ to a similar degree, that simultaneous inhibition can be reversed by PKA stimulation, and that this reversal of inhibition is attenuated by loss of CTD phosphorylation at S1700. We thus shed light on the regulation of the physiologically-relevant truncated forms of cardiac $Ca_V1.2$ by RAD and show that phosphorylation of the DCT and the GTPase can reconstitute PKA stimulation of the channel as co-regulators.

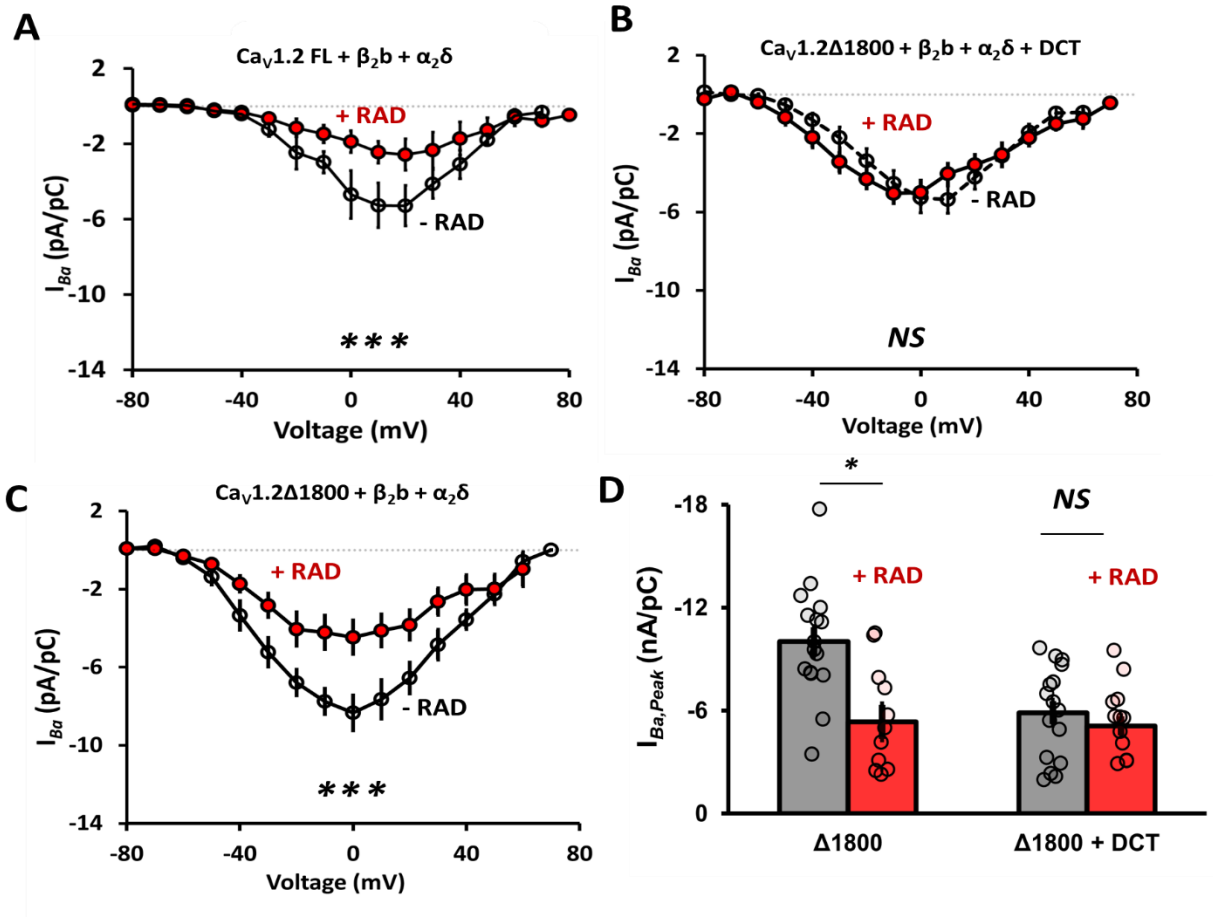

Figure 3.1. RAD Inhibits $Ca_V1.2\Delta1800$

IV curves of $Ca_V1.2\Delta1800$ co-expressed with (red) and without (black) RAD, in the full-length form (A), and the truncated form in the presence (**B**) and absence (**C**) of the DCT. (**D**) Peak current amplitudes observed during depolarized potentials between -10 mV and +10 mV. Statistical significance determined via ANOVA and Tukey HSD (FL and FL + RAD, *N* = 6 cells; Δ1800, N = 16; Δ1800 + RAD, N = 12; Δ1800 + DCT, N = 14; Δ1800 + DCT + RAD, N = 12).

3.1 RAD Inhibits $Ca_V1.2$ Δ1800 Current

Tsa-201 cells were transfected with $Ca_V1.2\Delta1800$, the auxiliary β_2b and $\alpha_2\delta$ subunits, the DCT, and RAD unless otherwise specified. The current-voltage relationship was determined via subsequent depolarizations at 10 mV intervals from resting membrane potential of -80 mV.

In cells transfected with $Ca_V1.2$ Δ1800 and RAD, we observed consistently depressed Ba^{2+} current when recording current-voltage (IV) relationships with a mean 44% lower peak current amplitude (-RAD: -10 ± 0.8 nA/pC, n = 16; +RAD: -5.6 ± 0.9 nA/pC, n = 11; p = 0.006) at depolarized potentials compared with cells without RAD (Fig. 3.1A, Fig. 3.1C). No significant shift in $V_{1/2}$ was observed.

When the DCT was co-transfected with $Ca_V1.2$ Δ1800, no additional IV or peak current suppression was observed in the presence of RAD (+DCT/-RAD: -5.5 ± 0.7 nA/pC, n = 14; +DCT/+RAD: -5.9 ± 0.7 nA/pC, n = 12; p = 0.90), revealing an absence of an "additive inhibition" of the already-autoinhibited $Ca_V1.2$ Δ1800 + DCT complex by RAD (Fig. 3.1B).

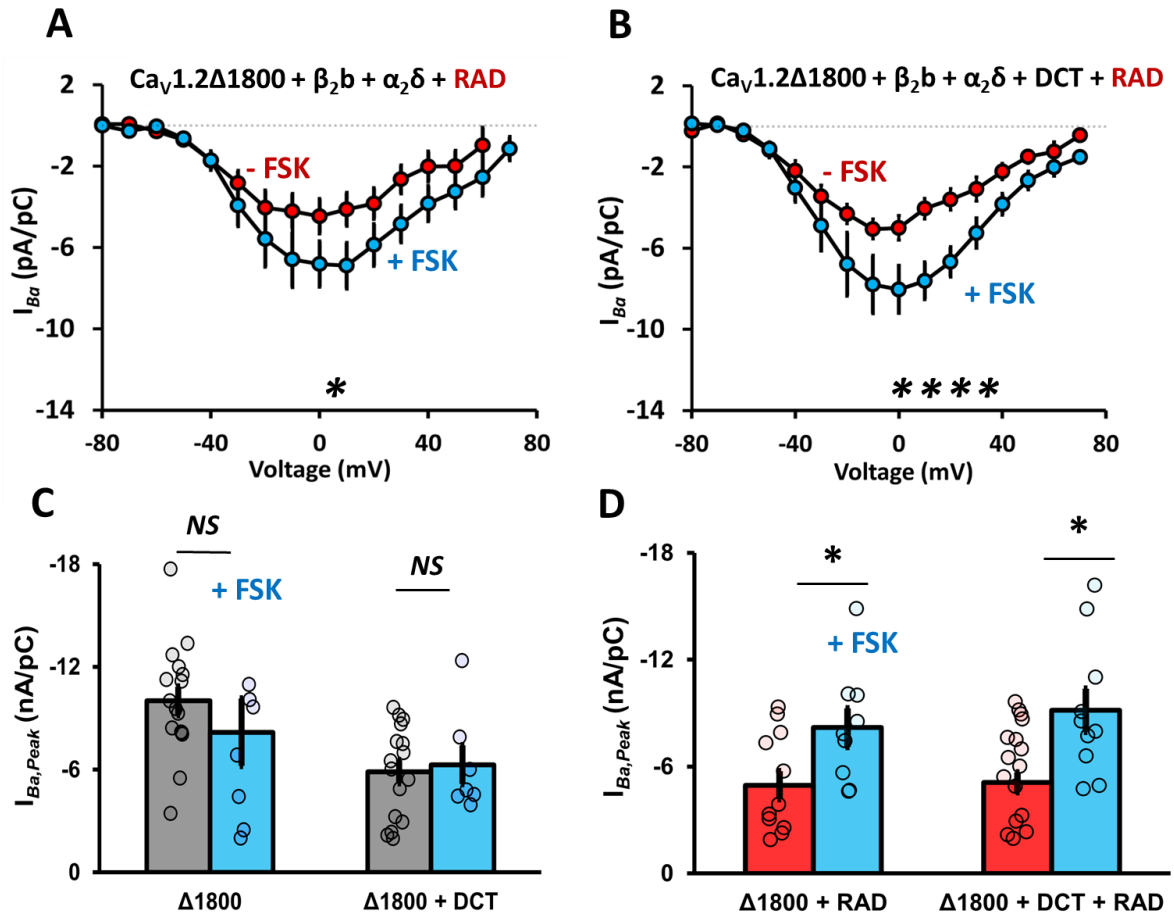

Figure 3.2. FSK Increases $Ca_V1.2$ Δ1800 Activity in the Presence of RAD

IV curves of FSK (blue) and non-FSK (red) treated cells $Ca_V1.2$Δ1800 co-expressed with RAD without (**A**) and with (**B**) the DCT. (**C**) Peak current amplitudes observed during depolarized potentials between -10 mV and +10 mV of cells expressing $Ca_V1.2$Δ1800 without and with the DCT in the absence of RAD, in the presence (blue) and absence (grey) of FSK. (**D**) Peak current amplitudes observed during depolarized potentials between -10 mV and +10 mV of cells co-expressing RAD and $Ca_V1.2$Δ1800 with and without the DCT, in the presence (blue) and absence (red) of FSK. Statistical significance determined via ANOVA and Tukey HSD. (Δ1800, *N* = 16 cells; Δ1800 + FSK, N = 8; Δ1800 + DCT, N = 14; Δ1800 + DCT + FSK, N = 10; Δ1800 + RAD, N = 12; Δ1800 + RAD + FSK, N = 9; Δ1800 + DCT + RAD, N = 12; Δ1800 + DCT + RAD + FSK, N = 10).

3.2 Forskolin Reverses RAD Inhibition of $Ca_V1.2$ Δ1800 + DCT

To evaluate PKA-dependent channel regulation of $Ca_V1.2$ Δ1800 and RAD, the adenylate-cyclase agonist forskolin (FSK) was added to the extracellular solution. Increased Ba^{2+} current was observed for both $Ca_V1.2$ Δ1800 (Fig. 3.2 A/C; - FSK: 5.6 ± 0.9 nA/pC, n = 11; + FSK: 8.3 ± 1.1 nA/pC, n = 9; p = 0.048) and $Ca_V1.2$ Δ1800 co-expressed with the DCT (Fig 3.2B/C- FSK: 5.5 ± 0.7 nA/pC, n = 12; +FSK: 9.2 ± 1.4 nA/pC, n = 10; p = 0.01) when RAD was present.

By contrast, in the absence of RAD co-expression, FSK did not lead to stimulation of $Ca_V1.2$ Δ1800 (Fig. 3.2C; -FSK: 10 ± 0.8 nA/pC, n = 16; +FSK: 8.2 ± 2 nA/pC, n = 8; p = 0.89) and $Ca_V1.2$ Δ1800 co-expressed with the DCT (-FSK: 5.9 ±0.7 nA/pC, n = 14; +FSK: 6.3 ± 1.1 nA/pC, n = 10; p = 0.22).

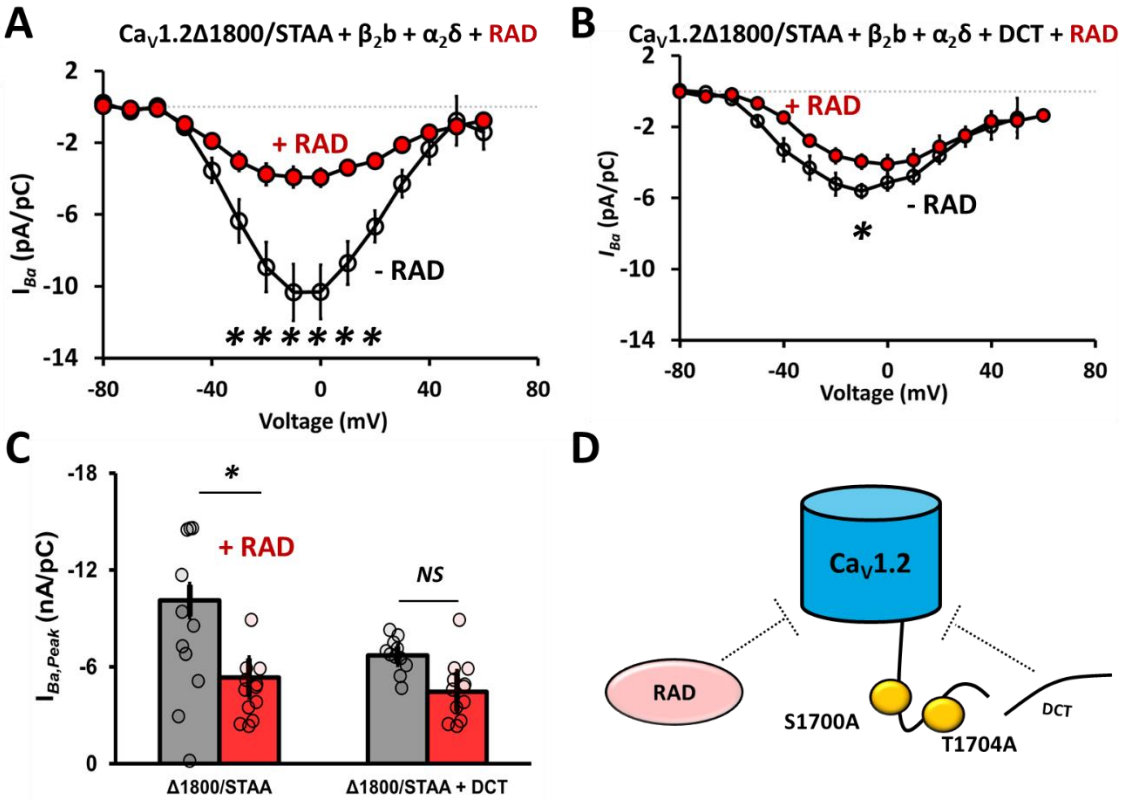

Figure 3.3. RAD Inhibits of Ca$_V$1.2 Δ1800 in Presence of CTD Phosphoregulatory Mutations

IV curves of Ca$_V$1.2Δ1800 with STAA phosphoregulatory with (red) and without (black) RAD co-expression, in the presence (**A**) and absence (**B**) of the DCT. (**C**) Peak current amplitudes observed during depolarized potentials between -10 mV and +10 mV. (**D**) Schematic showing S1700A and T1704 mutation sites, RAD and DCT inhibition. Statistical significance determined via ANOVA and Tukey HSD (Δ1800/STAA, *N* = 14 cells; Δ1800/STAA + DCT, N = 11; Δ1800/STAA + RAD, N = 12; Δ1800/STAA + DCT + RAD, N = 12).

3.3 FSK Stimulation Suppressed by CTD Phosphoregulatory Mutations

In order to determine whether loss of direct phosphorylation affected PKA-dependent regulation of the channel, we expressed mutant variants of Ca$_V$1.2 Δ1800 with either the Ser1700

(Δ1800/S1700A) position or the Ser1700 and Thr1704 (Δ1800/STAA; see Fig 3.3D for a schematic representation of the co-expression approach) positions mutated to alanine.

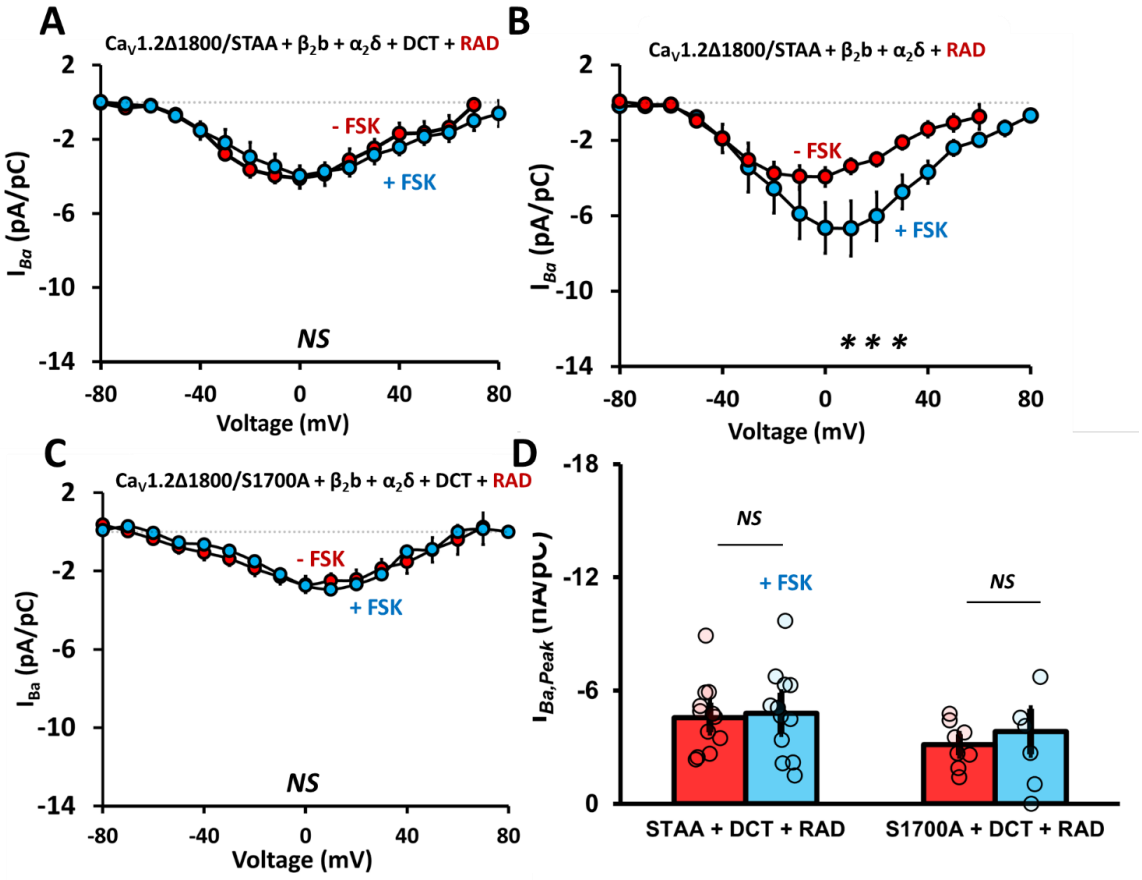

Figure 3.4. Stimulation of Cav1.2 Δ1800 in Presence of CTD Phosphoregulatory Mutations and RAD

IV curves of $Ca_V1.2\Delta1800$ with phosphoregulatory mutations with and without FSK exposure. (A) $Ca_V1.2\Delta1800$/STAA with DCT and RAD co-expression with and without FSK stimulation. (B) $Ca_V1.2\Delta1800$/STAA with RAD but without DCT co-expression with and without FSK stimulation. (C) CaV1.2Δ1800/S1700A with DCT and RAD co-expression with and without FSK stimulation. (D) Peak current amplitudes observed in cells expression $Ca_V1.2\Delta1800$/STAA and S1700A with and without FSK stimulation. Statistical significance determined via ANOVA and Tukey HSD (Δ1800/STAA + DCT + RAD, N = 12 cells; Δ1800/STAA + DCT + RAD + FSK, N

= 12; Δ1800/STAA + RAD, N = 12; Δ1800/STAA + RAD + FSK, N = 10; Δ1800/S1700A + DCT + RAD, N = 8; Δ1800/S1700A + DCT + RAD + FSK, N = 6).

As with WT $Ca_V1.2$ Δ1800, $Ca_V1.2$ Δ1800/STAA was robustly inhibited by (Fig. 3.3A, 3.3C ; -RAD: -10.1 ± 1.9 nA/pC, n = 14; +RAD: -4.5 ± 0.5 nA/pC, n = 12; p = 0.03). Unlike WT cells however, $Ca_V1.2$ Δ1800/STAA had depressed current at moderately depolarized voltages (between -40 mV and -10 mV) when the DCT and RAD were co-expressed. However, no statistically significant decrease in overall peak current was observed (Fig 3.3B/C; -RAD: -6.7 ± 0.3 nA/pC, n = 11; +RAD: -4.6 ± 0.5 nA/pC, n = 12; p = 0.22).

As observed for WT $Ca_V1.2$ Δ1800, $Ca_V1.2$ Δ1800/STAA also produced moderately increased current amplitudes in response to FSK (Fig. 3.4B; -FSK: 4.5 ± 0.5 nA/pC, n = 12; +FSK: 8.1 ± 1.7 nA/pC, n = 10; p = 0.04). Unlike the WT channels, however, in the presence of the DCT and RAD the $Ca_V1.2$ Δ1800/STAA, no FSK response was observed (Fig. 3.4A/C; -FSK: 4.6 ± 0.5 nA/pC, n = 12; +FSK: 4.8 ± 0.7 nA/pC, n = 12; p = 0.29) or altered IV characteristics. The single S1700A mutation also prevented the response FSK (Fig. 3.4C; -FSK: 3.1 ± 1 nA/pC, n = 8; +FSK: 3.8 ± 1 nA/pC, n = 5; p = 0.62).

These findings suggest that FSK stimulation of the truncated $Ca_V1.2$ is most robust in the presence of the DCT and RAD, and that loss of phosphorylation in the CTD blocks upregulation of channel activity. A proposed model for co-regulation of $Ca_V1.2$ Δ1800 by RAD, CTD phosphorylation, and the DCT is shown in Fig 3.6.

3.4 FSK Stimulation Suppressed by RAD Phosphoregulatory Mutations

Co-expression of a mutated, non-activatable RAD with 4 proposed PKA sites mutated to alanine, Ser25Ala, Ser38Ala, Ser272Ala, Ser300Ala (RAD_4M) with $Ca_V1.2$Δ1800 and the

DCT also resulted in a channel complex without increased activity in the presence of FSK (Fig. 3.5A/B; no FSK: -4 ± 1 pA/pC; + FSK: -4 ± 1 pA/pC, p = 1.0). Considering that the S1700A and STAA mutations also eliminated channel stimulation, these findings suggest that phosphorylation of both RAD and the CTD is necessary for robust upregulation by PKA of the $Ca_V1.2\Delta1800$ + DCT form of the channel. A schematic model representing these results is presented in Fig. 3.6

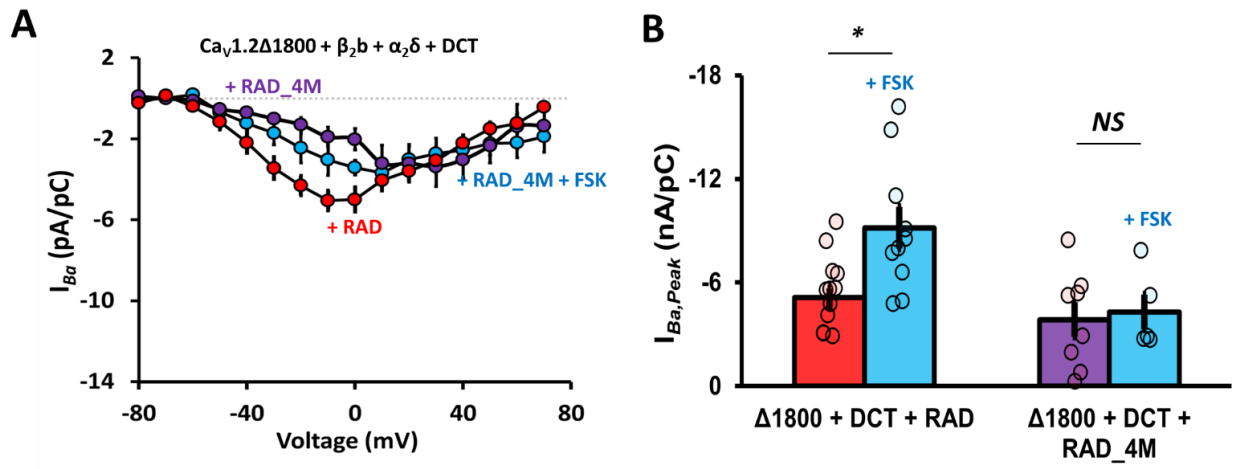

Figure 3.5. Stimulation of Ca$_V$1.2 Δ1800 in Presence of RAD with Phosphoregulatory Mutations

IV curves of $Ca_V1.2\Delta1800$ + DCT co-expressed with RAD with phosphoregulatory mutations (RAD_4M). (**A**) $Ca_V1.2\Delta1800$ with DCT and RAD_4M co-expression with and without FSK stimulation. (**B**) Peak current amplitudes observed in cells expressing of $Ca_V1.2\Delta1800$ + DCT with WT RAD and RAD_4M with and without FSK stimulation. Statistical significance determined via ANOVA and Tukey HSD (Δ1800 + DCT + RAD, *N* = 12 cells; Δ1800 + DCT + RAD + FSK, N = 12; Δ1800 + DCT + RAD_4M, N = 8; Δ1800 + DCT + RAD_4M, N = 5).

3.5 Broad Implications of $Ca_V1.2$ Co-Regulation by RAD And Direct Phosphorylation

As an essential therapeutic target for cardiac disorders ranging from chronic heart failure to tachyarrhythmias to post-myocardial infarction therapy, the cardiac fight-or-flight axis remains an important research area. Although significant effort has been made to elucidate the cardiac adrenergic signaling pathway, the detailed mechanism linking stimulation of cardiac β_1-adrenergic receptors to $Ca_V1.2$ and the excitation-contraction coupling apparatus remains elusive. Whereas several heterologous expression systems and animal models have demonstrated the critical role of the DCT and direct phosphorylation of the CTD in mediating forskolin or isoproterenol-induced upregulation of channel activity, studies in transgenic mice found preserved adrenergic response in the absence of direct $Ca_V1.2$ α-subunit phosphorylation.[32, 69] In heterologous tsa-201 cells, the requirement for co-expression of very specific concentrations of AKAP in order to observe stimulation of Cav1.2 current by forskolin has made reproducibility and interpretation of results in previous reconstitution studies difficult.[30] Our current study suggests that, in concert, RAD, the DCT, and direct phosphorylation of the CTD can give rise to robust PKA-dependent stimulation of $Ca_V1.2\Delta1800$, an important cardiac form of the channel.

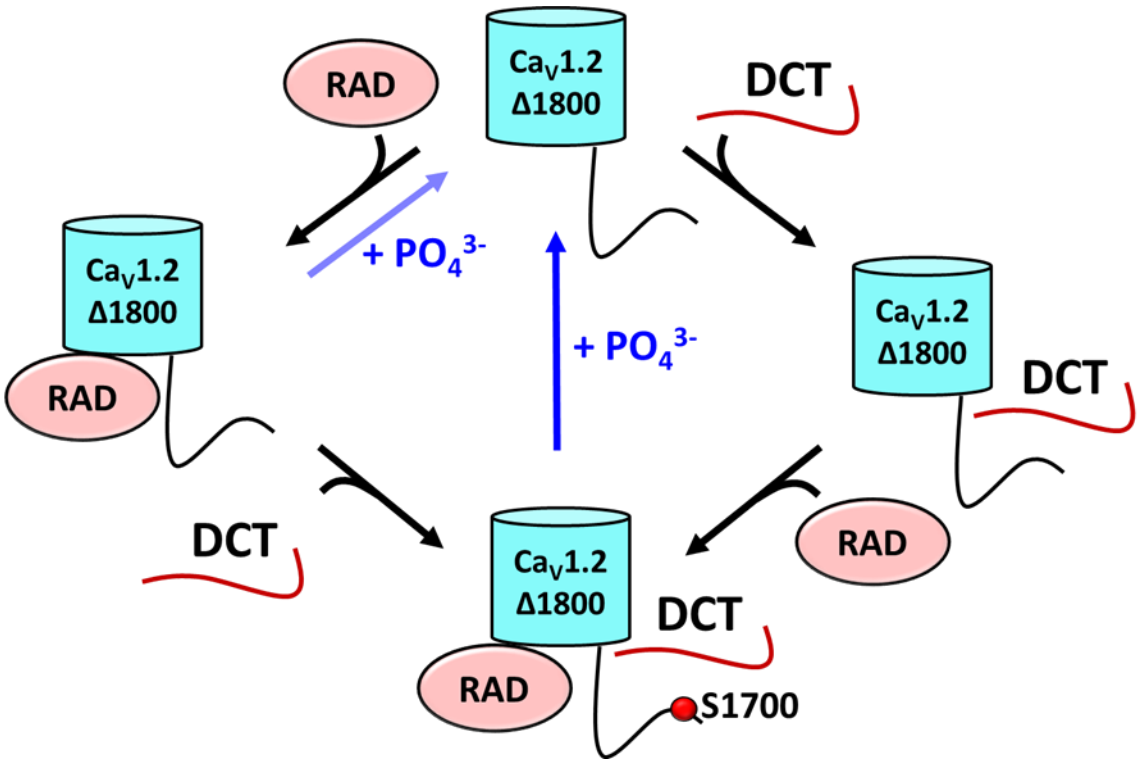

Figure 3.6. Model of Cav1.2Δ1800 Co-Regulation by RAD & DCT

Schematic diagram integrating $Ca_V1.2\Delta1800$ inhibition by RAD, the DCT, and CTD phosphorylation at S1700.

3.6 RAD and DCT as Co-inhibitors of $Ca_V1.2\Delta1800$

Previous work in both heterologous and transgenic mouse expression systems has primarily evaluated the regulation of full-length $Ca_V1.2$ by RAD.[33, 34] Whereas a portion of cardiac $Ca_V1.2$ in the heart is likely not proteolytically processed, the more abundant form is the truncated $Ca_V1.2\Delta1800$, likely in complex with the proteolyzed, auto-inhibitory DCT. Our findings indicate that while the presence of both RAD and DCT does not additionally inhibit peak channel current compared with either RAD or the DCT alone, the DCT did give rise to a more robust relative FSK stimulation than when the DCT was absent. This suggests that while the full-length channel

requires only RAD and phosphorylation of Ser1700 to reconstitute PKA stimulation, the $Ca_V1.2\Delta1800$ form of the channel is more effectively regulated by PKA by simultaneous DCT autoinhibition and RAD inhibition. Heterologous expression has shown that the DCT is critical for FSK upregulation of $Ca_V1.2$ current, and a mouse model with genetic deletion of the DCT was characterized by embryonic heart failure, further supporting the importance of this region of the channel in regulating normal cardiac function.

3.7 AKAP versus RAD-Mediated $Ca_V1.2$ Stimulation

Several AKAP (A-Kinase Anchoring Protein) have been shown to have important roles in the adrenergic regulation of $Ca_V1.2$. In mice, knockout of the AKAP Cypher/Zasp dramatically lowers isoproterenol-upregulated barium current in cardiomyocytes.[71] In tsa-201 cells, AKAP15 expressed in specific molar ratio with the $Ca_V1.2\Delta1800$ + DCT complex facilitates upregulation of the channel in the presence of FSK.[23, 30] In contrast with the RAD-dependent channel upregulation that we observe here, it has been previously shown that AKAP facilitates PKA stimulation without inhibiting either $Ca_V1.2\Delta1800$ or the $Ca_V1.2\Delta1800$ + DCT, suggesting a distinct role in mediating PKA regulation of the channel.[30]

3.8 Direct CTD Phosphorylation Required for Stimulation of Autoinhibited $Ca_V1.2$

We have presented here evidence that direct phosphorylation of the CTD is necessary for channel stimulation by FSK. The dual regulation of the autoinhibited $Ca_V1.2$ $\Delta1800$ form by direct phosphorylation and GTPase RAD supports the convergence of the RAD pathway and the DCT/direct phosphorylation pathways of the channel when PKA is activated. In the absence of

the autoinhibitory DCT, it appears that RAD alone is sufficient to mediate PKA-dependent upregulation of $Ca_V1.2$ Δ1800 activity.

Table 3.3. Peak I-V Current of $Ca_V1.2$ Variants Expressed with RAD

Construct	I_{Ba} (nA/pC) ± SEM	p-value$_{WT-FL}$	$I_{Ba,+FSK}$ (nA/pC) ± SEM	p-value$_{±FSK}$	$I_{Ba,RAD}$ (nA/pC) ± SEM	p-value$_{±RAD}$	$I_{Ba,RAD+FSK}$ (nA/pC) ± SEM	p-value$_{RAD±FSK}$
WT FL	-6 ± 1	n = 6			-3.0 ± 0.9	0.049; n = 6		
Δ1800 + DCT	-5.9 ± 0.7	0.99; n = 14	-6 ± 1	1.0; n = 10	-5.1 ± 0.5	0.89; n = 12	-9 ± 1	0.007; n = 10
Δ1800	-10.0 ± 0.8	0.094; n = 16	-8 ± 2	0.68; n = 8	-5.0 ± 0.8	< 0.001; n = 12	-8 ± 1	0.048; n = 9
Δ1800/STAA + DCT	-6.7 ± 0.3	0.92; n = 11			-4.6 ± 0.5	0.22; n = 12	-4.8 ± 0.7	1.0; n = 12
Δ1800/STAA	-10.1 ± 1.9	0.09; n = 14			-4.5 ± 0.5	0.03; n = 12	-8 ± 2	0.030; n = 10
Δ1800/SA + DCT					-3.1 ± 0.4	n = 8	-4 ± 1	0.35; n = 6
Δ1800 + DCT + RAD_4M					-4 ± 1	n = 8	-4 ± 1	1.0; n = 5

3.9 Co-Regulation by RAD and the DCT: Towards a Coherent Model of the Cardiac Fight-or-Flight Response

Over the past two decades, evidence has unfolded linking CTD proteolysis, DCT autoinhibition, CTD phosphorylation, β-subunit phosphorylation and trafficking, AKAP association, RAD phosphorylation, and several other factors to increased $Ca_V1.2$ activity following β-adrenergic stimulation. Although some inconsistencies and questions remain to be resolved, a unified mechanism involving the CTD, RAD, and $Ca_V\beta$ is emerging, with each piece likely contributing aspects of the adrenergic response in redundant, additive, antagonistic, or synergistic interactions that have yet to be fully elucidated.

An interesting possibility is that the partially preserved adrenergic response to high doses of isoproterenol that is observed in global S1700A and STAA mice (but not the conditional STAA

knock-in mouse), as well as the preserved adrenergic response of the transgenic phosphomutant mouse models might arise due to adaptive changes in the RAD pathway. We anticipate that advances in understanding of $Ca_V1.2$ regulation in the fight-or-flight response will help guide future work in the development novel inotropes, anti-hypertrophic medications, and next-generation neurohormonal blocking agents for cardiac disorders.

3.10 Conclusions on RAD and $Ca_V1.2$ CTD Phosphoregulation

We report here that the abundant cardiac Δ1800 form of $Ca_V1.2$ is inhibited by RAD and the channel DCT. We furthermore observed that the activity of this channel complex is stimulated by activation of PKA. Loss of phosphorylation at $Ca_V1.2$ position S1700 blunted PKA-mediated upregulation when both the DCT and RAD were present, but upregulation was preserved when the DCT was absent. Finally, we found that loss of phosphorylation of PKA sites on RAD also led to blunting of the PKA-dependent upregulation of CaV1.2, suggesting that both direct phosphorylation of $Ca_V1.2$ and of RAD are required for robust PKA-dependent regulation. Taken together, these findings strongly suggest PKA-dependent regulation of $Ca_V1.2Δ1800$ arises through the convergence of the autoinhibition/direct phosphorylation and RAD-mediated regulatory pathways.

Chapter 4. Regulation of Cardiac $Ca_V1.2$ by CaMKII

CaMKII is highly expressed in diverse tissue types and carries out important functions in intracellular calcium signaling throughout the central nervous system, immune system, and cardiac muscle.[52] Four genes give rise to the primary CaMKII isoforms (α, β, γ, δ) in humans, and alternative splicing generates multiple functionally distinct splice variants within each isoform.[72]

CaMKII has been shown to alter $Ca_V1.2$ current facilitation properties, increasing Ca^{2+} conduction during sequential depolarizations.[73] CaMKII signaling is of particular interest in the study of cardiac $Ca_V1.2$ phosphoregulation because 1) the kinase can phosphorylate canonical CaMKII phosphorylation sites at S1512 and S1570 *and* the PKA site S1700 in the $Ca_V1.2$ CTD, and 2) because CaMKII is highly involved in hypertrophy and pathologic remodeling.[23, 52, 54]

Increased expression and activity of the Ca^{2+}/calmodulin-dependent kinase II delta-isoform (CaMKII-δ), the predominant cardiac form of CaMKII, has been associated with cardiac hypertrophy and maladaptive remodeling in several heart failure models, and inhibition of the CaMKII signaling axis has been considered as a potential therapeutic target in CHF.[52, 72]

4.1 Increased Expression of CaMKII in $Ca_V1.2$ Phosphomutant Mice

Using qPCR and Western blotting, I observed that CaMKII-δ is expressed at markedly higher levels in young STAA mouse ventricular tissue compared with WT controls (Fig. 4.1A/B; normalized Western blot intensity; WT: 1.0 ± 0.3, STAA: 2.3 ± 0.6; $p = 0.007$). mRNA levels of the cardiac predominant CaMKII-δ and two of its splice variants, CaMKII-δ_C and CaMKII-δ_9, variants were also elevated significantly relative to age-matched WT controls (Fig 4.1C; expression fold-change R_Q: CaMKII-δ: 2.2 ± 0.3, $p = 0.037$; CaMKII-δ_C: 6 ± 3; $p = 0.041$; CaMKII-δ_C: : 5 ± 2; $p = 0.046$).

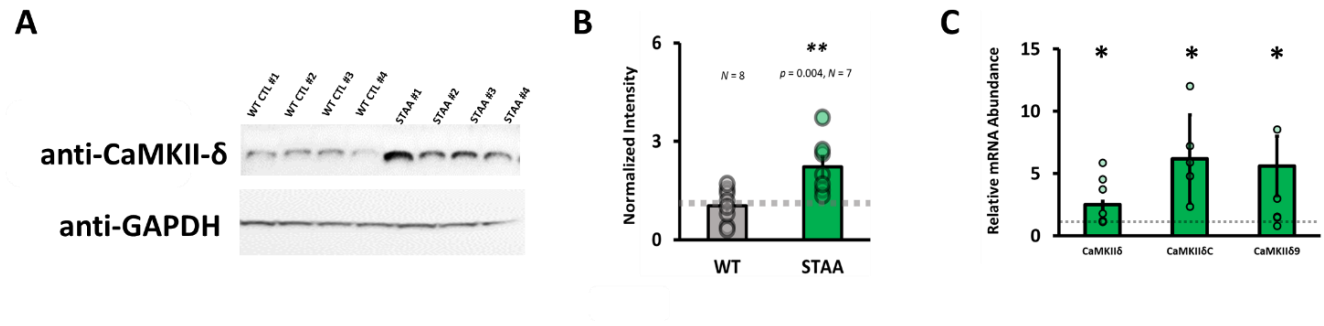

Figure 4.1. CaMKIIδ Expression is Elevated in Young STAA Mice.
(A) Western blot showing CaMKIIδ expression in ventricular lysate of 2-3 month old WT and STAA mice and (B) quantification of intensities from immunoblots normalized to anti-GAPDH. (C) mRNA expression of CaMKIIδ splice variant mRNA in young STAA mice relative to WT control animals.

4.2 Acute Blockade of CaMKII Increases Contractility In Mice

In order to evaluate the impact of pharmacologic CaMKII blockade on *in vivo* cardiac contractile function, I assessed the effect of 18 μg/kg intraperitoneal KN-93 administration in WT animals and $Ca_V1.2$ STAA mice aged 3-4 months during echocardiographic assessment of heart function. Most animals in both the WT and STAA cohorts experienced a modest increase in FS following administration of KN-93, but the effect was not statistically significant with ANOVA regression (Fig. 4.2A/Table 4.1; WT $FS_{Baseline}$: 28.5 ± 0.9%, WT FS_{KN-93}: 34 ± 2%, p = 0.44; STAA $FS_{Baseline}$: 17.2 ± 0.9%, WT FS_{KN-93}: 23 ± 3%, p = 0.18). There was also no significant alteration in heart rate following drug administration (Fig. 4.2B/Table 4.1; WT $HR_{Baseline}$: 449 ± 21 BPM, WT HR_{KN-93}: 477 ± 19 BPM, p = 0.79; STAA $HR_{Baseline}$: 515 ± 11 BPM, WT HR_{KN-93}: 516 ± 21 BPM, p = 1.0).

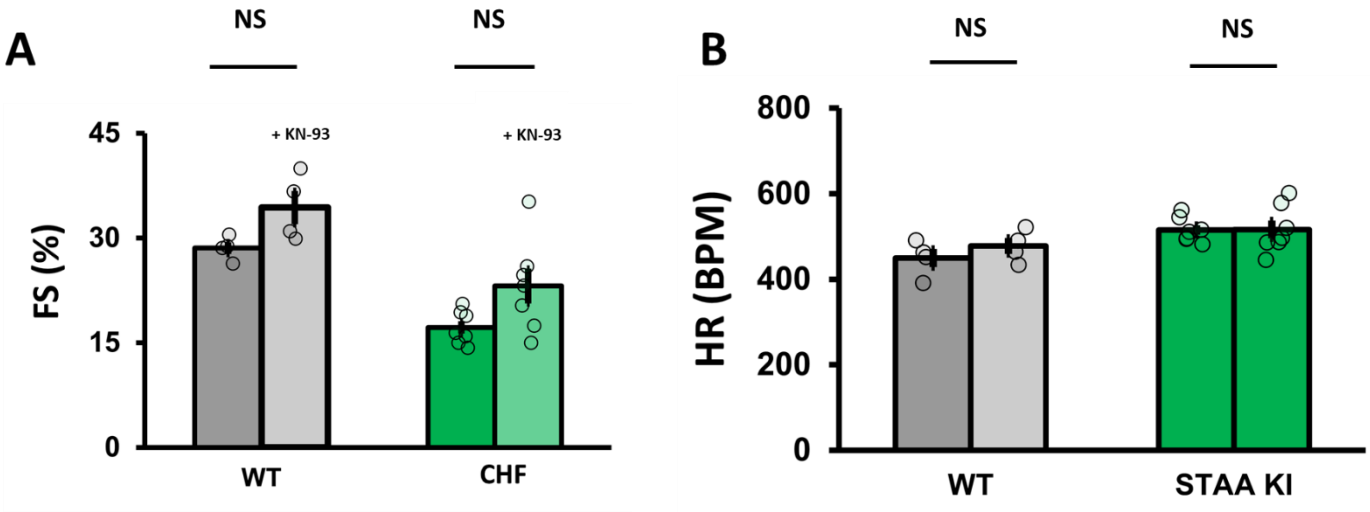

Figure 4.2. Acute Exposure to KN-93 in WT and $Ca_V1.2$ STAA Mice.

(A) FS and (B) HR before and after acute intraperitoneal KN-93 administration in WT and $Ca_V1.2$ STAA mice aged 4 – 5 months. Statistical significance determined via ANOVA and Tukey HSD (N = 4 mice for WT, N = 7 for STAA).

Table 4.4. Chronotropic and Inotropic Effects of Acute Administration of KN-93

	WT	**STAA**
Acute Administration		
$FS_{Baseline}$ ± SEM (%)	28.5 ± 0.8	17.2 ± 0.9
# Animals	N = 4	N = 7
p-value vs WT		0.001
FS_{KN-93} ± SEM (%)	34 ± 2	23 ± 3
p-value FS vs WT		0.0140
p-value FS vs Baseline	0.44	0.18
ΔFS ± SEM (%)	6 ± 2	6 ± 2
p-value FS vs WT		1.0

$HR_{Baseline}$ ± SEM (BPM)	449 ± 21	515 ± 11
p-value vs WT		0.10
HR_{KN-93} ± SEM (BPM)	477 ± 19	516 ± 21
p-value FS vs WT		0.49
p-value FS vs Baseline	0.79	1.0
ΔHR ± SEM (BPM)	34 ± 2	1 ± 19
p-value FS vs WT		0.23

4.3 Chronic Inhibition Of CaMKII Interacts with β-Adrenergic Blockade in $Ca_V1.2$ Phosphomutant Mice

To further evaluate the role of CaMKII regulation in the $Ca_V1.2$ STAA mice, which represent a slowly progressive age-dependent CHF model, I administered daily intraperitoneal 18 μg/kg KN-93 (a CaMKII inhibitor) to 8-week old $Ca_V1.2$ STAA mice for 1 month. Chronic inhibition of CaMKII by the antagonist KN-93 for 4 weeks in mutant STAA mice did not produce statistically significant changes in contractility compared with vehicle (Fig. 4.3A/Table 4.2; ΔFS Vehicle: -4 ± 2%; KN-93: 0 ± 1%, p = 0.16; KN-93/Bisoprolol: -5 ± 1%, p = 0.067). The combination of the β-blocker bisoprolol and KN-93, however, resulted in increased left-ventricular diameter (Fig. 4.3B/Table 4.2; $LVEDD_{Post}$ Vehicle: 4.5 ± 0.2 mm, p = 0.99, KN-93: 4.4 ± 0.1, p = 0.8; KN-93/Bisoprolol: 5.1 ± 0.1, p = 0.015).

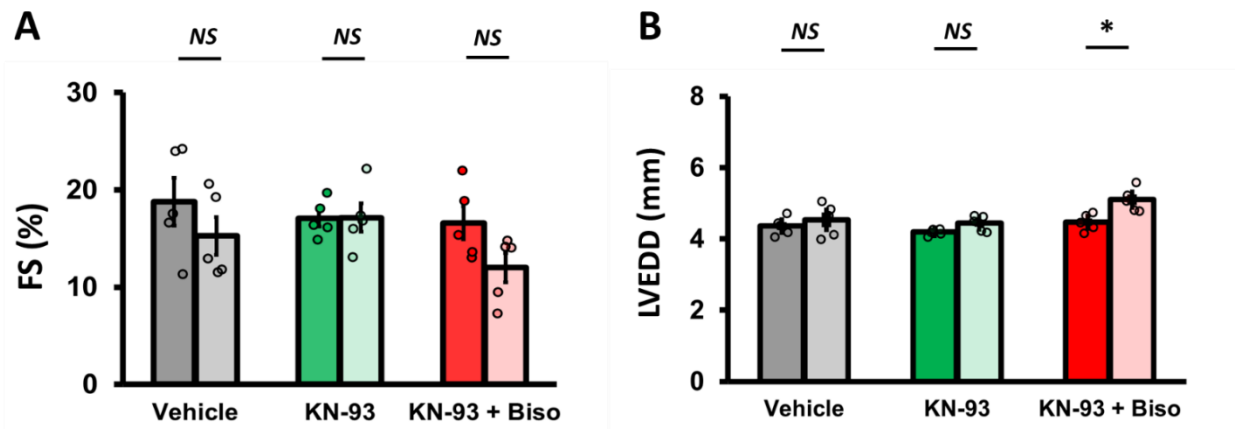

Figure 4.3. Chronic Exposure to KN-93 Increases Heart Volume when Co-Administered with Bisoprolol.

(A) FS and (B) LVIDD before and after 1 month of daily KN-93 administration in $Ca_V1.2$ STAA mice aged 4 – 5 months. Statistical significance determined via ANOVA and Tukey HSD (N = 5 mice for each condition).

4.4 CaMKII Interaction with Phosphoregulatory Mutations in the $Ca_V1.2$ CTD

My investigation into the intersection of cardiac CaMKII regulation and $Ca_V1.2$ phospho-regulation by PKA revealed a marked increase in CaMKII expression and CaMKII mRNA in mice with STAA mutations. This finding may be the consequence of a generalized hypertrophic stress response – since CaMKII is also elevated in several other mouse models of hypertrophy and the STAA mice have evidence of contractile dysfunction and ventricular dilation by 4 weeks of age or earlier.

The loss of phosphorylation of the $Ca_V1.2$ CTD may also have more direct effect on CaMKII levels, as CaMKII binds to the channel near the disrupted STAA phosphorylation sites.[74] Its function and expression may also be altered by changes in the calcium conduction activity of the mutant variant of $Ca_V1.2$, as CaMKII is activated by binding of Ca^{2+}-saturated calmodulin.[73] Nevertheless, the findings of markedly elevated subtypes of CaMKII ($CaMKII\delta_C$ and δ_9 splice

variants, which do not contain a nuclear localization sequence) in the slowly progressive $Ca_V1.2$ STAA model of heart failure motivates further investigation into whether inhibition of the excess CaMKII would further impair cardiac function of protect against pathologic remodeling. Since CaMKII has been shown to readily phosphorylate some PKA sites on $Ca_V1.2$ in *in vitro* mass spectrometric studies, I anticipated that blocking the enzyme acutely with KN-93 would result in lower FS. Inhibition of CaMKII with 18 mg/kg KN-93 – a dose range often used in the literature – did not produce decreased FS, however, and even resulted in a trend towards increased contractility in both WT and $Ca_V1.2$ STAA mice.[75, 76]

A small experimental study evaluating the effect of daily administration of KN-93 to $Ca_V1.2$ STAA mice for one month revealed no statistically significant alteration in FS or left-ventricular volume in the KN-93 mice compared with animals that received vehicle. There was a trend towards *attenuated* loss of FS and less ventricular dilation in the KN-93 group, but the effect was modest and would likely require a much larger cohort to generate statistically significant differences. A third cohort of mice received bisoprolol, a β_1-adrenergic receptor antagonist, to assess the impact of combining KN-93 with a "standard-of-care" heart failure drug that has shown efficacy in preventing remodeling mice that received TAC.[70] Interestingly, the mice that received bisoprolol and KN-93 experienced a statistically significant increase in left-ventricular volume, suggesting that hypertrophic changes were exacerbated when both the CaMKII and β-adrenergic pathways were blocked (see Fig. 4.3C).

KN-93 inhibits all variants of CaMKII, including those in vascular smooth muscle, so interpretation of these results in terms of effects on cardiac function is difficult.[72] Additional studies should be performed evaluating the interaction of CaMKII inhibition with β-adrenergic

antagonists, as we observed a worsening in cardiac parameters when bisoprolol and KN-93 were combined.

4.1 Conclusions On the Impact of $Ca_V1.2$ CTD Phosphoregulatory Mutations on CaMKII Signaling

Additional mechanistic studies on the $Ca_V1.2$ phosphoregulation by CaMKII and PKA are required to better understand how these signaling pathways simultaneously regulate $Ca_V1.2$ under resting cardiac conditions and during the fight-or-flight response. We have shown that expression of cardiac variants of CaMKII is sharply elevated, even at young ages, in ventricular muscle from STAA mice, that acute blockade of CaMKII does not decrease (and may even increase) contractility, and that combining chronic adrenergic and CaMKII blockade exacerbates cardiac remodeling in STAA mice.

Table 4.2. Functional and Morphologic Consequences of Long-Term KN-93 Administration in Mice with $Ca_V1.2$ Phosphoregulatory Mutations

	Vehicle	**KN-93**	**KN-93 + Bisoprolol**
Chronic Administration			
$FS_{Baseline}$ ± SEM (%)	19 ± 2	17 ± 1	17 ± 2
# Animals	N = 5	N = 5	N = 5
p-value vs WT		0.70	1.0
FSK_{Post} ± SEM (%)	15 ± 2	17 ± 1	12 ± 1
p-value FS vs Vehicle		0.59	0.33
p-value FS vs Baseline	0.37	1.0	0.16

ΔFS ± SEM (%)	-4 ± 2	0 ± 1	-5 ± 1
p-value FS vs Vehicle		0.16	0.067
$LVEDD_{Baseline}$ ± SEM (mm)	4.4 ± 0.1	4.19 ± 0.04	4.5 ± 0.1
p-value vs WT		0.23	0.69
$LVEDD_{Post}$ ± SEM (mm)	4.5 ± 0.2	4.4 ± 0.1	5.1 ± 0.1
p-value FS vs Vehicle		0.87	0.011
p-value FS vs Baseline	0.99	0.80	0.015
$LVESD_{Baseline}$ ± SEM (mm)	3.6 ± 0.2	3.5 ± 0.1	3.7 ± 0.1
p-value FS vs Vehicle		1.0	1.0
$LVESD_{Post}$ ± SEM (mm)	3.9 ± 0.3	3.7 ± 0.1	4.5 ± 0.2
p-value FS vs Vehicle		1.00	0.22
p-value FS vs Baseline	0.85	0.97	0.05

Chapter 5. Materials And Methods

The materials and methods used in Chapters 2-4 of this work are described in this section.

5.1 Animal Models

C57BL/6 mice expressing Ala at amino acid positions 1700, 1700 and 1704, or 1928 and their WT littermate controls were used in the study. Experimental procedures were approved by the Institutional Animal Care and Use Committee of University of Washington and all studies were carried out in accordance with the approved guidelines. Evenly balanced cohorts of female and male mice were used, and ages are described individually for each experiment, but animals were generally between the ages of 4 – 15 weeks at the time the experiments were conducted.

5.2 Echocardiography

Echocardiography was performed with a VisualSonics Vevo 2100 imaging system under light isoflurane sedation as described previously.[77]

5.3 Transverse Aortic Constriction

The surgical procedure for transverse aortic constriction (TAC) was performed as described previously.[77]

5.4 Heart Weight

Mice were weighed, euthanized, and the hearts were isolated. The whole heart was briefly rinsed in PBS to remove blood. The hearts were blotted dry, separated into ventricle and atrium, and weighed. Ventricular weight was subsequently normalized to mouse bodyweight.

5.5 β-Agonist Administration

A racemic mixture of isoproterenol (Sigma-Aldrich #I6504) dissolved in 0.9% saline was used for this study. After baseline echocardiographic assessment, S1700A, STAA, or S1928A mice aged 5-15 weeks were given 0.25 - 100 μg/kg isoproterenol via intraperitoneal injection. Post-injection echocardiographic measurements were made two minutes after drug administration.

5.1 KN-93 Administration

KN-93 (MedChemExpress #139298) was dissolved in vehicle solution (10% DMSO, 40% PEG300, 5% Tween-80, 45% saline). For the acute studies, the drug was injected intraperitoneally following baseline assessment of cardiac parameters and subsequent measurements were made 4

minutes after drug administration. In the chronic exposure study, cardiac parameters were assessed in 4 - 5 month old STAA mice at baseline, followed by daily administration of 18 mg/kg KN-93 for 30 days. A follow-up echocardiographic assessment was subsequently performed.

5.2 Quantification of Cardiac Hypertrophic Markers

Ventricular cardiac tissue was isolated from mice 4 weeks after TAC surgery and from littermate controls who did not receive surgery. Total cDNA libraries were generated using RNA isolation and reverse transcription. Quantitative PCR was performed using primers for ANP (fwd: 5'-TCGTCTTGGCCTTTTGGCT-3', rev: 5'-TCC AGG TGG TCT AGC AGG TTC T-3'), BNP (fwd: 5'- AAGTCCTAGCCAGTCTCCAGA-3, rev: 5'- GAG CTG TCT CTG GGC CAT TTC -3'), β-MHC (fwd: 5'-ATGTGCCGGACCTTGGAAG-3', rev: 5'-CCT CGG GTT AGC TGA GAG ATC A-3'), and GAPDH (fwd: 5' CAT GGC CTT CCG TGT TCC TA 3', rev: 5' CCT GCT TCA CCA CCT TCT TGA T 3'). Normalized amplification threshold (ΔCT) values were measured for each sample relative to GAPDH control reaction. ΔΔCT was calculated as the difference in ΔCT between post-TAC and non-TAC animals, and expression fold change (RQ) was calculated via the logarithmic transformation $2^{-\Delta\Delta CT}$.

5.3 Cell Culture and Transfection

Tsa-201 cells were transfected as previously described with rat $Ca_V1.2$ Δ1800 (residues 1-1800), the β_2b subunit, the $\alpha_2\delta$ subunit, the DCT (1801-2122), and RAD pcDNA3.1 plasmids in a 1:1:1:0.75:1 molar ratio unless otherwise specified.

5.4 Electrophysiology

48 hours after transfection cells were immersed extracellular solution containing 10 mM Ba^{2+}, 1mM $MgCl_2$, voltage-clamped at -80 mV using 3-5 MΩ glass electrodes with 50-70% series resistance compensation. A -p/4 leak subtraction protocol was applied to each recording and current amplitudes during each depolarization were normalized to gating charge. Peak currents were determined as the largest current amplitude observed during any depolarization recorded at 10 mV intervals ranging from -80 mV to + 80 mV. For stimulated cell recordings, 10 μM FSK was added to extracellular buffer and cells, followed by a 10 minute equilibration before recording.

5.5 Immunoblotting

Western blots were carried out as previously described. Anti-CaMKIIδ antibody (ProteinTech Group #15443) was used in 1:500 dilution during primary incubation.

5.6 Statistical Analysis

Data are shown as means ± SEM of number of measurements performed. Statistical significance was tested with Student's t test for pairwise analysis, and analysis of variance (ANOVA) followed by Tukey's test for comparison of multiple conditions.

BIBLIOGRAPHY

1. Shimizu H, Okabe M. Evolutionary origin of autonomic regulation of physiological activities in vertebrate phyla. *Journal of Comparative Physiology A*. 2007/10/01 2007;193(10):1013-1019.

2. Lymperopoulos A, Rengo G, Koch WJ. Adrenergic nervous system in heart failure: pathophysiology and therapy. *Circulation research*. 2013;113(6):739-753.

3. Cybulski N. O funkcyi nadnercza. *Gazeta Lekarska*. 1895;12:299-308.

4. Vincent S. On the General Physiological Effects of Extracts of the Suprarenal Capsules. *The Journal of physiology*. 1897;22(1-2):111-120.

5. Myrtle AS. Adrenalin in Neurotic Heart. *British medical journal*. 1904;1(2261):1009-1009.

6. Brown JC, Simons E, Rudders SA. Epinephrine in the Management of Anaphylaxis. *J Allergy Clin Immunol Pract*. Apr 2020;8(4):1186-1195.

7. Vargas M, Buonanno P, Iacovazzo C, Servillo G. Epinephrine for out of hospital cardiac arrest: A systematic review and meta-analysis of randomized controlled trials. *Resuscitation*. Mar 2019;136:54-60.

8. Nawrocki PS, Poremba M, Lawner BJ. Push Dose Epinephrine Use in the Management of Hypotension During Critical Care Transport. *Prehosp Emerg Care*. Mar-Apr 2020;24(2):188-195.

9. Powell CE, Slater IH, LeCompte L, Waddell JE. BLOCKING OF INHIBITORY ADRENERGIC RECEPTORS BY A DICHLORO ANALOG OF ISOPROTERENOL. *Journal of Pharmacology and Experimental Therapeutics*. 1958;122(4):480.

10. Harrison DC, Griffin JR, Fiene TJ. EFFECTS OF BETA-ADRENERGIC BLOCKADE WITH PROPRANOLOL IN PATIENTS WITH ATRIAL ARRHYTHMIAS. *N Engl J Med*. Aug 19 1965;273:410-5.

11. Dézsi CA, Szentes V. The Real Role of β-Blockers in Daily Cardiovascular Therapy. *Am J Cardiovasc Drugs*. Oct 2017;17(5):361-373.

12. Weiss S, Oz S, Benmocha A, Dascal N. Regulation of cardiac L-type Ca^{2+} channel CaV1.2 via the β-adrenergic-cAMP-protein kinase A pathway: old dogmas, advances, and new uncertainties. *Circulation Research*. 2013/08/16/ 2013;113(5):617-631.

13. Grzybowski A, Pietrzak K. Napoleon Cybulski (1854-1919). *J Neurol*. Nov 2013;260(11):2942-3.

14. Durães Campos I, Pinto V, Sousa N, Pereira VH. A brain within the heart: A review on the intracardiac nervous system. *J Mol Cell Cardiol*. Jun 2018;119:1-9.

15. Wallace AG, Sarnoff SJ. EFFECTS OF CARDIAC SYMPATHETIC NERVE STIMULATION ON CONDUCTION IN THE HEART. *Circ Res*. Jan 1964;14:86-92.

16. Ahlquist RP. A study of the adrenotropic receptors. *Am J Physiol*. Jun 1948;153(3):586-600.

17. Otsuka M. [Effects of adrenalin on Purkinje's fibers in mammalian hearts]. *Pflugers Arch Gesamte Physiol Menschen Tiere*. 1958;266(5):512-7. Die Wirkung von Adrenalin auf Purkinje-Fasern von Säugetierherzen.

18. Reuter H. Exchange of calcium ions in the mammalian myocardium. Mechanisms and physiological significance. *Circ Res*. May 1974;34(5):599-605.

19. Reuter H. Localization of beta adrenergic receptors, and effects of noradrenaline and cyclic nucleotides on action potentials, ionic currents and tension in mammalian cardiac muscle. *J Physiol*. 1974;242:429-451.

20. Tsien RW, Giles W, Greengard P. Cyclic AMP mediates the effects of adrenaline on cardiac purkinje fibres. *Nat New Biol*. Dec 6 1972;240(101):181-3.

21. Anderson ME. Totally Rad? The Long and Winding Road to Understanding CaV1.2 Regulation. *Circulation Research*. 2021/01/08 2021;128(1):89-91.

22. Emrick MA, Sadilek M, Konoki K, Catterall WA. β-adrenergic-regulated phosphorylation of the skeletal muscle $Ca_V1.1$ channel in the fight-or-flight response. *Proc Natl Acad Sci U S A*. Oct 26 2010;107(43):18712-7.

23. Fuller MD, Emrick MA, Sadilek M, Scheuer T, Catterall WA. Molecular mechanism of calcium channel regulation in the fight-or-flight response. *Sci Signal*. 2010;3(141):ra70.

24. Hulme JT, Konoki K, Lin TW, et al. Sites of proteolytic processing and noncovalent association of the distal C-terminal domain of CaV1.1 channels in skeletal muscle. *Proc Natl Acad Sci U S A*. Apr 5 2005;102(14):5274-5279.

25. Hulme JT, Yarov-Yarovoy V, Lin TW-C, Scheuer T, Catterall WA. Autoinhibitory control of the Cav1.2 channel by its proteolytically cleaved distal C-terminal domain. *J Physiol (Lond)*. 2006;576:87-102.

26. Hulme JT, Westenbroek RE, Scheuer T, Catterall WA. Phosphorylation of serine 1928 in the distal C-terminal of cardiac Cav1.2 channels during β-adrenergic regulation. *Proc Natl Acad Sci U S A*. 2006;103:16574-16579.

27. Fu Y, Westenbroek RE, Yu FH, et al. Deletion of the Distal C Terminus of CaV1.2 Channels Leads to Loss of β-Adrenergic Regulation and Heart Failure in Vivo. 2011 2011;286(14):11.

28. Fu Y, Westenbroek RE, Scheuer T, Catterall WA. Phosphorylation sites required for regulation of cardiac calcium channels in the fight-or-flight response. *Proc Natl Acad Sci U S A*. Nov 26 2013;110(48):19621-6. doi:10.1073/pnas.1319421110

29. Fu Y, Westenbroek RE, Scheuer T, Catterall WA. Basal and β-adrenergic regulation of the cardiac calcium channel $Ca_V1.2$ requires phosphorylation of serine 1700. *Proc Natl Acad Sci U S A*. Nov 18 2014;111(46):16598-603.

30. Fuller MD, Fu Y, Scheuer T, Catterall WA. Differential regulation of CaV1.2 channels by cAMP-dependent protein kinase bound to A-kinase anchoring proteins 15 and 79/150. *J Gen Physiol*. Mar 2014;143(3):315-24. doi:10.1085/jgp.201311075

31. AA P, DD C, P S, HM C. Similar molecular determinants on Rem mediate two distinct modes of inhibition of Ca V 1.2 channels. *Channels (Austin, Tex)*. 09/02/2016 2016;10(5)

32. Katchman A, Yang L, Zakharov SI, et al. Proteolytic cleavage and PKA phosphorylation of α1C subunit are not required for adrenergic regulation of CaV1.2 in the heart. *Proceedings of the National Academy of Sciences of the United States of America*. 2017//08/22 2017;114(34):9194-9199.

33. G L, A P, AN K, et al. Mechanism of adrenergic Ca V 1.2 stimulation revealed by proximity proteomics. *Nature*. 2020 Jan 2020;577(7792)

34. A P, J K, JA H, et al. Adrenergic Ca V 1.2 Activation via Rad Phosphorylation Converges at α 1C I-II Loop. *Circulation research*. 01/08/2021 2021;128(1)

35. Fu Y, Westenbroek RE, Scheuer T, Catterall WA. Phosphorylation sites required for regulation of cardiac calcium channels in the fight-or-flight response. *Proceedings of the National Academy of Sciences*. 2013/11/26/ 2013;110(48):19621-19626.

36. Hulme JT, Lin TW, Westenbroek RE, Scheuer T, Catterall WA. β-adrenergic regulation requires direct anchoring of PKA to cardiac $Ca_V1.2$ channels via a leucine zipper interaction with A kinase-anchoring protein 15. *Proc Natl Acad Sci U S A*. 2003;100(22):13093-13098.

37. Fu Y, Westenbroek RE, Scheuer T, Catterall WA. Basal and β-adrenergic regulation of the cardiac calcium channel CaV1.2 requires phosphorylation of serine 1700. *Proceedings of the National Academy of Sciences*. 2014/11/18/ 2014;111(46):16598-16603.

38. Yang L, Dai D-F, Yuan C, et al. Loss of β-adrenergic–stimulated phosphorylation of CaV1.2 channels on Ser1700 leads to heart failure. *Proceedings of the National Academy of Sciences*. 2016/12/06/ 2016;113(49):E7976-E7985.

39. Poomvanicha M, Matthes J, Domes K, et al. Beta-adrenergic regulation of the heart expressing the Ser1700A/Thr1704A mutated Cav1.2 channel. *Journal of Molecular and Cellular Cardiology*. 2017/10/01/ 2017;111:10-16.

40. Qian H, Patriarchi T, Price JL, et al. Phosphorylation of Ser1928 mediates the enhanced activity of the L-type Ca2+ channel Cav1.2 by the beta2-adrenergic receptor in neurons. *Sci Signal*. Jan 24 2017;10(463)

41. Nystoriak MA, Nieves-Cintrón M, Patriarchi T, et al. Ser1928 phosphorylation by PKA stimulates the L-type Ca2+ channel CaV1.2 and vasoconstriction during acute hyperglycemia and diabetes. *Science Signaling*. 2017//01/24 2017;10(463)

42. Lemke T, Welling A, Christel CJ, et al. Unchanged β-Adrenergic Stimulation of Cardiac L-type Calcium Channels in Cav1.2 Phosphorylation Site S1928A Mutant Mice. *Journal of Biological Chemistry*. 2008/12/12/ 2008;283(50):34738-34744.

43. De Jongh KS, Murphy BJ, Colvin AA, Hell JW, Takahashi M, Catterall WA. Specific phosphorylation of a site in the full-length form of the α1 subunit of the cardiac L-type calcium channel by adenosine 3',5'-cyclic monophosphate-dependent protein kinase. *Biochemistry*. Aug 13 1996;35(32):10392-402.

44. Catterall WA, Hulme JT, Jiang X, Few WP. Regulation of sodium and calcium channels by signaling complexes. *Journal of Receptor and Signal Transduction Research*. 2006 2006;26(5-6):577-598.

45. Fu Y, Westenbroek RE, Yu FH, et al. Deletion of the distal C terminus of CaV1.2 channels leads to loss of β-adrenergic regulation and heart failure in vivo. Apr 8 2011;286(14):12617-26.

46. Yang L, Dai DF, Yuan C, et al. Loss of beta-adrenergic-stimulated phosphorylation of $Ca_V1.2$ channels on Ser1700 leads to heart failure. *Proceedings of the National Academy of Sciences*. 2016;109.

47. Brunet S, Emrick MA, Sadilek M, Scheuer T, Catterall WA. Phosphorylation sites in the Hook domain of CaVβ subunits differentially modulate CaV1.2 channel function. *J Mol Cell Cardiol*. Oct 2015;87:248-56.

48. Buraei Z, Yang J. Inhibition of voltage-gated calcium channels by RGK proteins. Research Support, N.I.H., Extramural. *Curr Mol Pharmacol*. 2015;8(2):180-7.

49. BS F, SM C, J S, DA A. Regulation of voltage-gated calcium channel activity by the Rem and Rad GTPases. *Proceedings of the National Academy of Sciences of the United States of America*. 11/25/2003 2003;100(24)

50. Katz M, Subramaniam S, Chomsky-Hecht O, et al. Reconstitution of β-adrenergic regulation of $Ca_V1.2$: Rad-dependent and Rad-independent protein kinase A mechanisms. *Proceedings of the National Academy of Sciences*. 2021;118(21):e2100021118.

51. BM A, BM L, S V, et al. Myocardial-restricted ablation of the GTPase RAD results in a pro-adaptive heart response in mice. *The Journal of biological chemistry*. 07/12/2019 2019;294(28)

52. Bers DM. CaMKII inhibition in heart failure makes jump to human. *Circ Res*. Oct 29 2010;107(9):1044-6.

53. Koval OM, Guan X, Wu Y, et al. CaV1.2 beta-subunit coordinates CaMKII-triggered cardiomyocyte death and afterdepolarizations. *Proc Natl Acad Sci U S A*. Mar 16 2010;107(11):4996-5000.

54. Sossalla S, Fluschnik N, Schotola H, et al. Inhibition of elevated Ca2+/calmodulin-dependent protein kinase II improves contractility in human failing myocardium. *Circ Res*. Oct 29 2010;107(9):1150-61.

55. Blaich A, Welling A, Fischer S, et al. Facilitation of murine cardiac L-type Ca(v)1.2 channel is modulated by calmodulin kinase II-dependent phosphorylation of S1512 and S1570. *Proc Natl Acad Sci U S A*. Jun 1 2010;107(22):10285-9.

56. Eom GH, Cho YK, Ko J-H, et al. Casein Kinase-2α1 Induces Hypertrophic Response by Phosphorylation of Histone Deacetylase 2 S394 and its Activation in the Heart. *Circulation*. 2011/05/31 2011;123(21):2392-2403.

57. Kashihara T, Nakada T, Kojima K, Takeshita T, Yamada M. Angiotensin II activates Ca(V) 1.2 Ca(2+) channels through β-arrestin2 and casein kinase 2 in mouse immature cardiomyocytes. *J Physiol*. Jul 1 2017;595(13):4207-4225.

58. Virani SS, Alonso A, Benjamin EJ, et al. Heart Disease and Stroke Statistics—2020 Update: A Report From the American Heart Association. *Circulation*. 2020/03/03 2020;141(9):e139-e596.

59. Murphy SP, Ibrahim NE, Januzzi JL, Jr. Heart Failure With Reduced Ejection Fraction: A Review. *JAMA*. 2020/08/04/ 2020;324(5):488-504.

60. de Lucia C, Eguchi A, Koch WJ. New Insights in Cardiac β-Adrenergic Signaling During Heart Failure and Aging. *Frontiers in Pharmacology*. 2018/08/10/ 2018;9

61. Goldstein RE, Boccuzzi SJ, Cruess D, Nattel S, Adverse Experience C, Multi Diltiazem Postinfarction Res G. Diltiazem increases late-onset congestive heart failure in postinfarction patients with early reduction in ejection fraction. *Circulation*. 1991;83:52-60.

62. Liao P, Soong TW. $Ca_V1.2$ channelopathies: from arrhythmias to autism, bipolar disorder, and immunodeficiency. *Pflugers Arch*. Jul 2010;460(2):353-359.

63. Zhang Q, Chen J, Qin Y, Wang J, Zhou L. Mutations in voltage-gated L-type calcium channel: implications in cardiac arrhythmia. *Channels (Austin, Tex)*. 2018 2018;12(1):201-218.

64. Splawski I, Timothy KW, Decher N, et al. Severe arrhythmia disorder caused by cardiac L-type calcium channel mutations. *Proc Natl Acad Sci U S A*. Jun 7 2005;102(23):8089-96; discussion 8086-8.

65. Splawski I, Timothy KW, Sharpe LM, et al. $Ca_V1.2$ calcium channel dysfunction causes a multisystem disorder including arrhythmia and autism. *Cell*. Oct 1 2004;119(1):19-31.

66. Fu Y, Westenbroek RE, Yu FH, et al. Deletion of the Distal C Terminus of CaV1.2 Channels Leads to Loss of β-Adrenergic Regulation and Heart Failure in Vivo. *The Journal of Biological Chemistry*. 2011/04/08/ 2011;286(14):12617-12626.

67. Riehle C, Bauersachs J. Small animal models of heart failure. *Cardiovascular research*. 2019;115(13):1838-1849.

68. Kvetnansky R, Kubovcakova L, Tillinger A, Micutkova L, Krizanova O, Sabban EL. Gene expression of phenylethanolamine N-methyltransferase in corticotropin-releasing hormone knockout mice during stress exposure. *Cell Mol Neurobiol*. Jul-Aug 2006;26(4-6):735-54.

69. Yang L, Katchman A, Samad T, Morrow JP, Weinberg RL, Marx SO. β-adrenergic regulation of the L-type Ca2+ channel does not require phosphorylation of α1C Ser1700. *Circ Res*. Sep 13 2013;113(7):871-80.

70. Xiang S, Zhang N, Yang Z, Bian Z, Yuan Y, Tang Q. Achievement of a target dose of bisoprolol may not be a preferred option for attenuating pressure overload-induced cardiac hypertrophy and fibrosis. *Experimental and Therapeutic Medicine*. 2016/10/01/ 2016;12(4):2027-2038.

71. H Y, C Y, RE W, WA C. The AKAP Cypher/Zasp contributes to β-adrenergic/PKA stimulation of cardiac Ca V 1.2 calcium channels. *The Journal of general physiology*. 06/04/2018 2018;150(6)

72. Pellicena P, Schulman H. CaMKII inhibitors: from research tools to therapeutic agents. *Frontiers in pharmacology*. 2014;5:21-21.

73. Bers DM, Morotti S. Ca(2+) current facilitation is CaMKII-dependent and has arrhythmogenic consequences. *Frontiers in pharmacology*. 2014;5:144-144.

74. Hudmon A, Schulman H, Kim J, Maltez JM, Tsien RW, Pitt GS. CaMKII tethers to L-type Ca2+ channels, establishing a local and dedicated integrator of Ca2+ signals for facilitation. *J Cell Biol*. Nov 7 2005;171(3):537-47.

75. Wu Y, Temple J, Zhang R, et al. Calmodulin kinase II and arrhythmias in a mouse model of cardiac hypertrophy. *Circulation*. Sep 3 2002;106(10):1288-93.

76. Zhong P, Quan D, Huang Y, Huang H. CaMKII Activation Promotes Cardiac Electrical Remodeling and Increases the Susceptibility to Arrhythmia Induction in High-fat Diet–Fed Mice With Hyperlipidemia Conditions. *Journal of Cardiovascular Pharmacology*. 2017;70(4)

77. Li L, Guo X, Chen Y, et al. Assessment of Cardiac Morphological and Functional Changes in Mouse Model of Transverse Aortic Constriction by Echocardiographic Imaging. *Journal of Visualized Experiments : JoVE*. 2016/06/21/ 2016;(112)

VITA

Liam Hovey grew up in Kiel, Germany, and received B.S. degrees in Physics, Chemistry, and Biochemistry, with a minor in Mathematics from the University of Iowa in Iowa City. In 2015, he matriculated into the Medical Scientist Training Program at the University of Washington, Seattle. Liam is interested in cardiovascular physiology and pharmacology, heart failure, arrhythmias, and oncology.